CRCLEME
Cooperative Research Centre for Landscape Environments and Mineral Exploration

action Salinity & Water AUSTRALIA

Government of South Australia

OPEN FILE REPORT SERIES

CSIRO

Australian Government Geoscience Australia

OTBC

CONSTRAINED INVERSION OF RESOLVE ELECTROMAGNETIC DATA - RIVERLAND, SOUTH AUSTRALIA

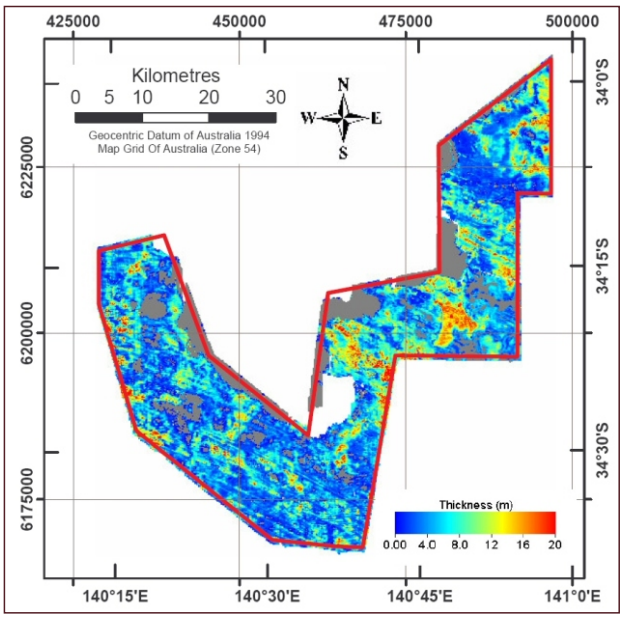

R. Brodie, A. Green and T. Munday

CRC LEME OPEN FILE REPORT 175

September 2004

CONSTRAINED INVERSION OF RESOLVE ELECTROMAGNETIC DATA - RIVERLAND, SOUTH AUSTRALIA

R. Brodie, A. Green and T. Munday

CRC LEME OPEN FILE REPORT 175

September 2004

Report prepared for the South Australia Salinity Mapping and Management Support Project.
This project is jointly funded by the South Australian and Commonwealth Governments under the National Action Plan for Salinity and Water Quality.

CRC LEME is an unincorporated joint venture between CSIRO-Exploration & Mining, and Land and Water, The Australian National University, Curtin University of Technology, University of Adelaide, Geoscience Australia, Primary Industries and Resources SA, NSW Department of Mineral Resources and Minerals Council of Australia.

Headquarters: CRC LEME c/o CSIRO Exploration and Mining, PO Box 1130, Bentley WA 6102, Australia

Copies of this Publication can be obtained from :
The publications Officer, CRCLEME, c/- CSIRO Exploration and Mining, PO Box 1130, Bentley WA 6120, Australia. Information on other publications in this series may be obtained from the above, or from http://crcleme.org.au
Cataloguing-in-Publication:
Name: Brodie, R., Green, A. and Munday, T. Title: Constrained inversion of RESOLVE airborne electromagnetic data – Riverland, South Australia.
ISBN 1 921039 13 2
1. Riverland, South Australia 2. AEM 3. Constrained Inversion
I. Name II. Title
CRCLEME Open File Report 175
ISSN 1329-4768

Address and Affiliation of Authors

Ross Brodie
Geoscience Australia
GPO Box 378,
Canberra, ACT 2601
Australia

Andy Green
OTBC Pty. Ltd
8 Lawley Cres.
Pymble NSW 2073
Australia

Tim Munday
Cooperative Research Centre for Landscape Environments and Mineral Exploration
c/- CSIRO Exploration and Mining
26 Dick Perry Avenue,
Technology Park,
Kensington, Western Australia 6151
Australia.

PREFACE AND EXECUTIVE SUMMARY

This report describes a subset of activities undertaken CRCLEME as part of contribution to the Riverland and Tintinara projects of the South Australia Salinity Mapping and Monitoring Project conducted under the auspices of The National Action Plan for Salinity and Water Quality (NAP). Specifically, it concerns the development of constrained inversion methodologies to invert RESOLVE helicopter EM data in order to map the location and thickness of near-surface clay-rich materials. In the Riverland region, the focus of this report, these materials are principally associated with the Blanchetown Clay sedimentary unit. The Blanchetown clay, and units of like texture, act to delay the rate of groundwater recharge and thus locations where it is present are more favourable for agricultural development.

After a preliminary analysis to select the optimum system and survey characteristics, approximately 12,000 line-km were surveyed in the Riverland region at line spacings of 150 or 300 m. The data were recalibrated with measurements from down-hole induction logs and then inverted using a 1-D layered-earth model. In order to improve the sensitivity to the unknown aspects of the ground section, the inversion was constrained with as much local geological and hydrological information as possible. These constraints included information about the depth of the water table, the conductivity of the groundwater, the variability of the conductivity and thickness of two sand units. An understanding of the geological and geomorphic history of the area was also used to help define the probable geometry, distribution and disposition of relevant sedimentary units.

A map of the distribution and thickness of the Blanchetown Clay and like-units was generated. The results of the inversion also allowed us to reconstruct the beach strandline-dominated palaeo-topography left when the sea retreated from the Murray Basin in the early Pliocene. They also can be used to define the landscape left after the demise of Lake Bungunnia. This latter surface, defined by the top of the Blanchetown Clay, is a complicated result of fluvial and aeolian redistribution processes that have, in some locations, reworked clays to positions well above the maximum level of the lake.

The survey also revealed a hitherto unsuspected, deeper variability in conductivity following the Pliocene strand line pattern. The cause of this pattern is not, as yet, clear

There are a number of potential uses for a detailed map of the distribution of the Blanchetown Clay. At present it is being used to model the recharge behaviour of the area as an input into a model predicting the future course of salinity inflows to the Murray River. If more areas are to be released for irrigation, the map could also be used to select areas of thicker clay that may be preferred locations for irrigation. Finally, areas of thicker clay are might also be the preferred location for disposal of saline water from salt interception schemes

Dr. Tim Munday
Project Leader
December 2003

CONTENTS

FIGURES

TABLES

ABSTRACT

The RESOLVE frequency domain HEM system has been used to map the distribution of near-surface clay-rich sediments, including the Blanchetown Clay, in and around the Riverland irrigation districts of South Australia.

After a preliminary analysis to select the optimum system and survey characteristics, approximately 12,000 line-km was surveyed at line spacings of 150 or 300 m. The data were recalibrated with measurements from down-hole induction logs and then inverted using a 1-D layered-earth model. In order to improve the sensitivity to the unknown aspects of the section, the inversion was constrained with as much local geological and hydrologeological information as possible. These constraints included information about the depth of the water table, the conductivity of the groundwater, the variability of the conductivity and thickness of three sedimentary units, and the geomorphic history of the area.

The results of the inversion allow us to reconstruct the strandline-dominated paleo-topography left when the sea retreated from the Murray Basin in the Early Pliocene. They also can be used to define the landscape left after the demise of Lake Bungunnia. This latter surface, defined as the top of the Blanchetown Clay, is further complicated as a result of fluvial and aeolian processes that have, in some locations, reworked and redistributed clays to positions well above the maximum level of the lake.

The resulting detailed map of the distribution of the Blanchetown Clay can be used in a variety of ways.

- It can be used to model the recharge behaviour of the area, which in turn can be used to help predict the future course of salinity inflows to the River Murray.
- If more areas are to be released for irrigation, the map could be used to select areas of thicker clay that are preferred locations for such developments.
- Areas of thicker clay are also preferred locations for disposal of saline water from salt interception schemes.

The survey also revealed a hitherto unsuspected, deeper variability in conductivity following the Pliocene strand line pattern. The cause of this pattern is not clear. It could be due to variation in the porosity of Loxton Sands or to strandline-correlated variability in the elevation of the contact between the Bookpurnong Beds and the Lower Loxton sands.

1. INTRODUCTION

This is the final report for the Constrained Inversion Project, a subproject of the Commonwealth Riverland and Tintinara projects which form part of the South Australia-Salinity Mapping and Management Support Project, funding under the National Action Plan for Salinity and Water Quality (NAPSWQ). The project developed and applied constrained inversion methodologies to invert RESOLVE helicopter airborne electromagnetic data (HEM) data to map the spatial distribution and thickness of a near surface conductor for a 15 km wide zone of the Riverland region in South Australia. This map was intended to serve as a surrogate for the distribution and variability of clay rich units (including the Blanchetown Clay), from which estimates of groundwater recharge can be defined, when used in conjunction with soil hydrological models.

An improved understanding of the distribution of the Blanchetown Clay and other clay rich materials in the near surface is important because they are perhaps the only sediments in the area that can impede groundwater recharge which has resulted from the clearing of deep-rooted, perennial native vegetation or from irrigation. Such recharge causes the water table to rise increasing the subsurface flow towards the River Murray. In many places this groundwater is very saline and increased salt loads into the Murray are the result.

Much of the study area has already been cleared and significant parts have been developed for irrigated agriculture. These changes are already having a significant impact on the river salinity levels. Further, assuming the availability of water, there will be continual pressure to open more land for irrigation. If this eventuates, it will have an even greater impact on the recharge. However if irrigation can be located in areas of lower hydraulic conductivity the onset of this enhanced recharge could be delayed considerably. Modelling studies (Cook *et.al*., 2001) of the likely future salinity levels in the Murray has stressed the need for improved information on the hydraulic conductivities in the area and this study has been designed to contribute to this objective.

In the future it is also clear that this section of the Murray will also be the subject of more salt interception schemes. These pumping schemes extract saline groundwater before it reaches the river and dispose of it in evaporation basins a safe distance from the river. Clearly, the evaporation basins must be located where recharge will be as low as possible and the same hydraulic conductivity considerations will apply as in the selection of new irrigation areas. In addition to disposal issues, the correct location of the pumping stations in zones of high permeability is critical to the efficiency of these schemes and, although it was not a major objective of this project, it was hoped that the regional geophysical overview might provide information that could inform the development of these schemes.

In early 2001, the above considerations and the potential availability of support through the National Action Plan for Salinity and Water Quality led to preliminary studies on the selection of the optimum AEM system for mapping the Blanchetown Clay. This work, (Munday *et.al*. 2003) that involved modelling studies and a small test survey, confirmed the ability of the RESOLVE system to detect the presence or absence of the Blanchetown Clay and the full survey was conducted as a result.

1.1 Location

The study area is a 10 to 15 kilometre wide zone following along the southern bank of the River Murray in South Australia.

The zone stretches between Kingston-On-Murray in the west to Wilperna Island north east of Renmark in the east. Longitudes 140º13'36"E and 140º58'04"E bound the area as do latitudes 33º57'37"S and 34º38'29"S specified relative to the Geocentric Datum of Australia coordinate system. Some 170,400 hectares are enclosed within the study area.

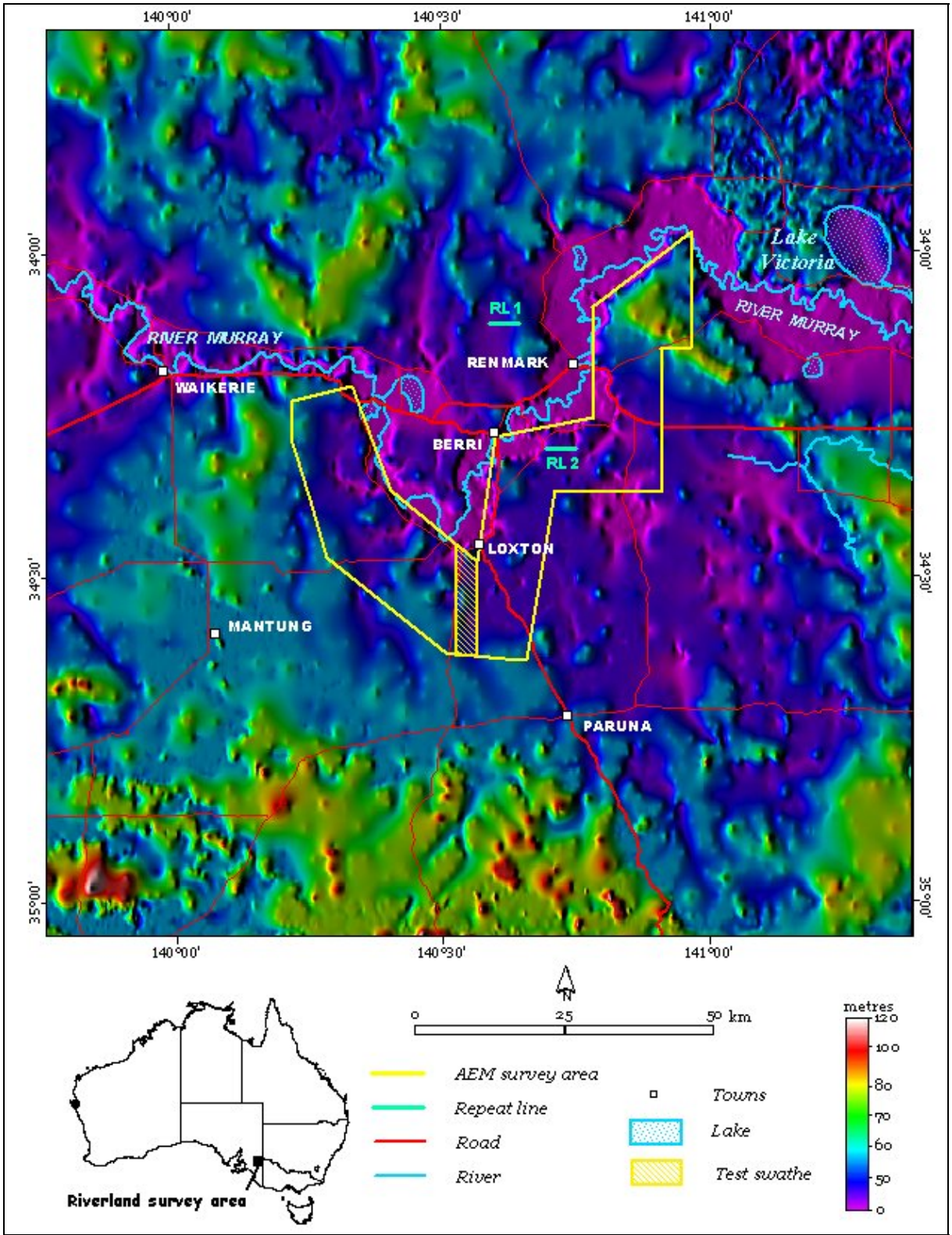

Figure 1. A DEM of the Riverland study area in South Australia. The RESOLVE Airborne Electromagnetic Survey area lies within the yellow polygon.

1.2 Geology and Geomorphology

The study area is located in the lower part of the Murray Basin, a roughly circular basin consisting of up to 600m of flat-lying Cainozoic sediments, which overlie various Palaeozoic and Mesozoic rocks (Brown and Stephenson, 1991). The basin is flanked by a series of subdued mountain ranges and hills.

The Cainozoic history of the basin has been characterised by slow relative subsidence, minimal compaction, and low rates of sedimentation, with the sedimentary succession forming an extensive, but relatively thin sequence over a tectonically active platform which was subject to partial inundation by epicontinental seas (Brown 1985). These marine transgressions, correlated with global sea level changes at various times during the Tertiary, and related environments of deposition, resulted in a range of sedimentary units including limestones, shelf muds, marine and beach sands, estuarine clays, alluvial sands and aeolian dunes. The final depositional cycle in the Basin was initiated by a rapid marine transgression at the end of the Miocene. Highstand deposition followed throughout the Pliocene leading to the progradation of the Loxton-Parilla sands – a composite assembly of (regressive) shoreface, beach, estuarine, dune, back-barrier lagoonal facies sediments that extend across a substantial part of the basin ((Stephenson, 1986, Roy et al, 2000). Parts of the Loxton-Parilla Sands are underlain by marine shelf muds, the Bookpurnong beds, that may be contemporaneous with the development of the regressive sand-barrier sequences. If this were the case, this unit would represent a low energy, offshore component of the prograding barrier system.

In the mid-Pliocene, barrier progradation stalled with the uplift of the Pinaroo Block and Padthaway ridge (Roy et al., 2000, Sandiford, 2003) to the south of the study area. Drainage was impounded leading to the development of a large lake known as Lake Bungunnia (Stephenson, 1986) some 33,000km^2 in area. Deposition of fine-grained lacustrine and flvio-lacustrine sediments followed, referred to collectively as the Blanchetown Clay. Stephenson (1986) described this unit as "a greenish grey, red-brown or variegated sandy clay with many local variations in lithology" and has been reported as blanketing the swales between Loxton-Parilla sand barriers (Colwell 1977). The Blanchetown Clay unit is commonly only a few metres thick but can reach 20m in isolated instances. In the study area the Blanchetown Clay has been mapped in drill holes and is known to occur on current topographic highs.

Increased aridity during the Quaternary precipitated the demise of Lake Bungunnia. This was accompanied by the aeolian reworking of the clays and associated surficial sediments into mobile, East-West oriented, sand sheets that form the Woorinen formation and the Molineaux-Lowan Sands. These younger sediments are commonly up to 5m thick, though they may exceed 20m in some dunes. Fluvial activity in the region was limited to the main rivers and their margins. Both the aeolian and fluvial processes are believed to have affected present-day topography. Besides influencing the development of an East-West dune system, aeolian processes have deflated the Blanchetown Clay in places, resulting in localised topographic lows with only the Loxton-Parilla sands remaining.. In the central part of the basin, including the Riverland region, the maximum height of the Blanchetown Clay is at 60mAHD (Kotsonis, 1999, Stephenson, 1986). As a consequence, it is thought that, aside from landforms associated with recent aeolian activity, the current topography reflects that of the late Pliocene quite accurately.

The elevation of most of the study area ranges from 30 to 65 metres above sea level. It is only in the most northerly part of the area where the elevation is above the postulated maximum elevation of Lake Bungunnia (~60m AHD) . Here a prominent NW-SW trending ridge rises to 85 m. Recent research (Roy et al, 2000, Sandiford 2003a,b), suggests that localised faulting and uplift was active through the Pliocene and into the Quaternary. It is possible that this ridge and elevated ground around Bookpurnong, north of Loxton may be related to uplifted fault blocks. On the floodplain of the River Murray the elevation drops to 10m

The surface elevation derived from the airborne data is shown in Figure 2. The high spatial frequency, E-W sand dune pattern is obvious but in the southern arm of the survey area it is possible to discern a NW-SE pattern that is somewhat wider spaced than the dunes. This is a topographic expression of the Pliocene strandline pattern and although it often represents only a few meters elevation difference the spatial coherence of the pattern makes it discernable.

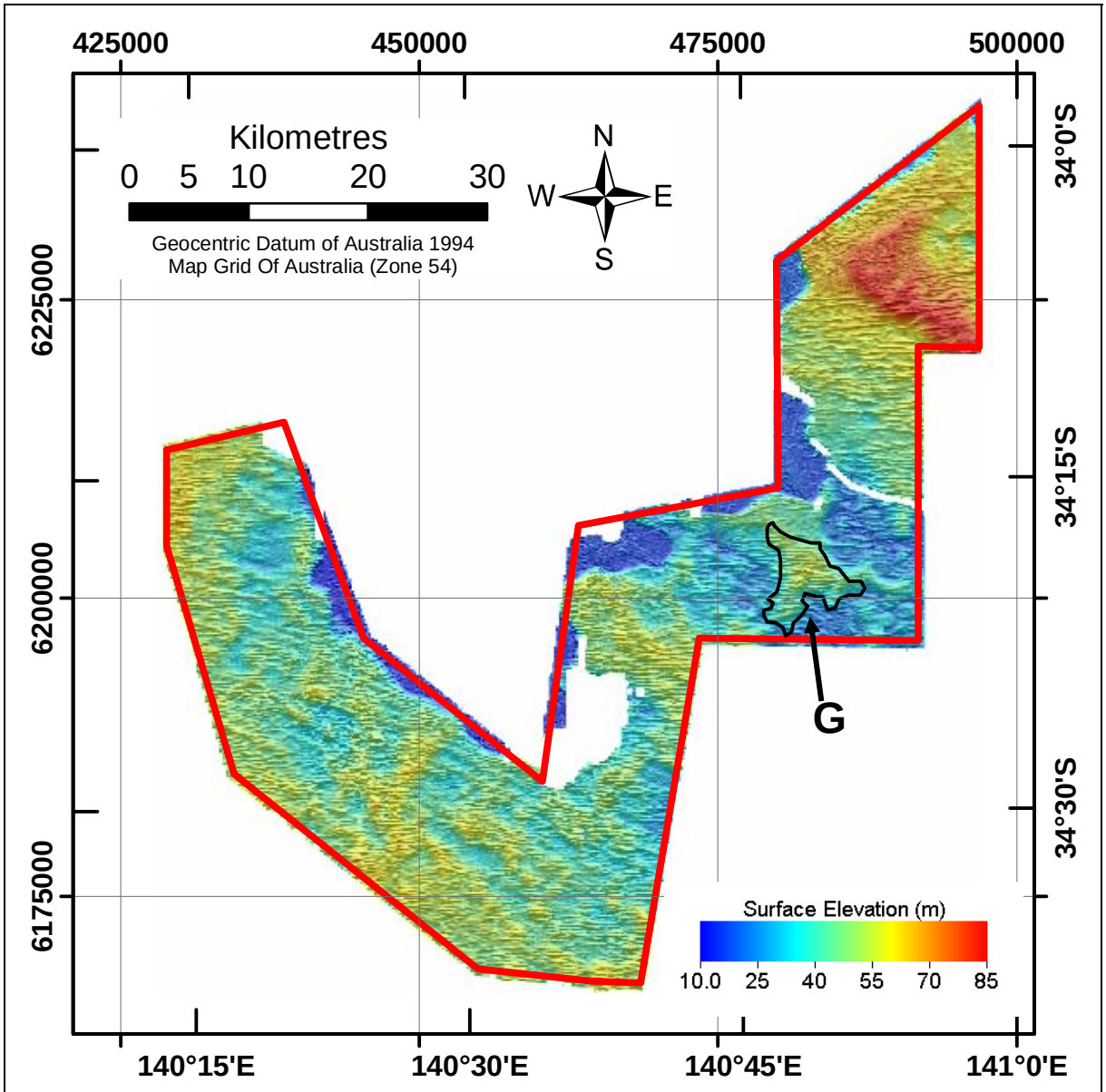

Figure 2.: Surface elevation derived from the AEM survey. Note certain areas within the polygon were not flown due to aviation regulations preventing flying in built up areas and over major highways. The area G, outlined by a black polygon was subject to special processing and is discussed later.

The groundwater in the survey area has been well characterized by extensive drilling. The images below (Figures 3 and 4) show the result of griding data supplied by DWLBC.

In the groundwater elevation data, the most obvious feature is an irrigation-induced groundwater mound around Loxton. Otherwise the water table elevation varies quite slowly with a small gradient from East to West and, locally, towards the river. An area of high conductivity between Loxton and the Stuart Highway dominates the groundwater conductivity image. Here, shallow, highly saline groundwater flows west towards the Murray beneath an area of, generally, low elevation.

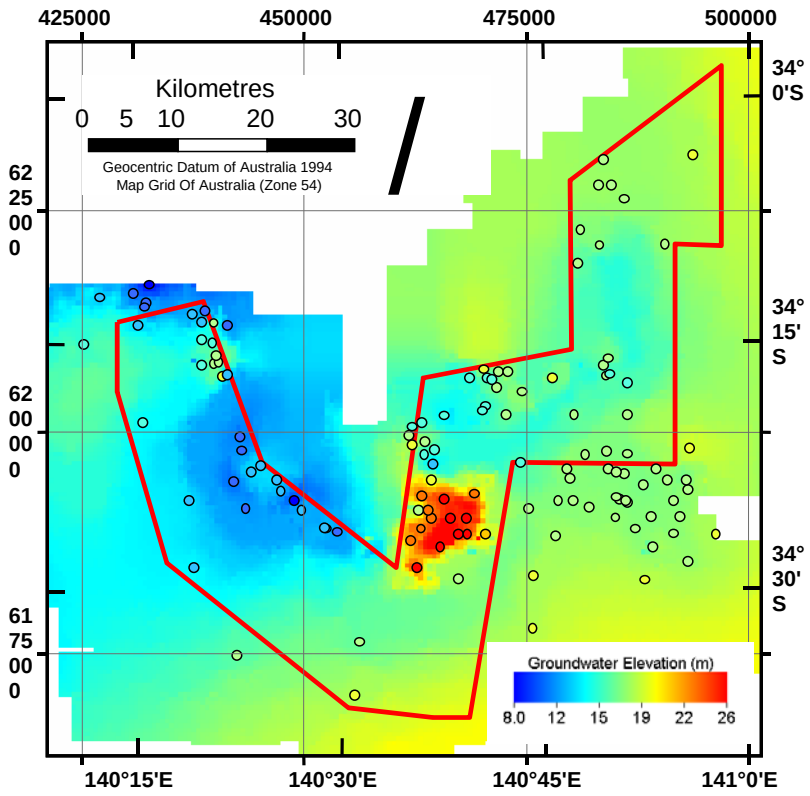

Figure 3.: Elevation of the groundwater above sea level. Circles represent the locations of the bores from which groundwater elevation observations were made.

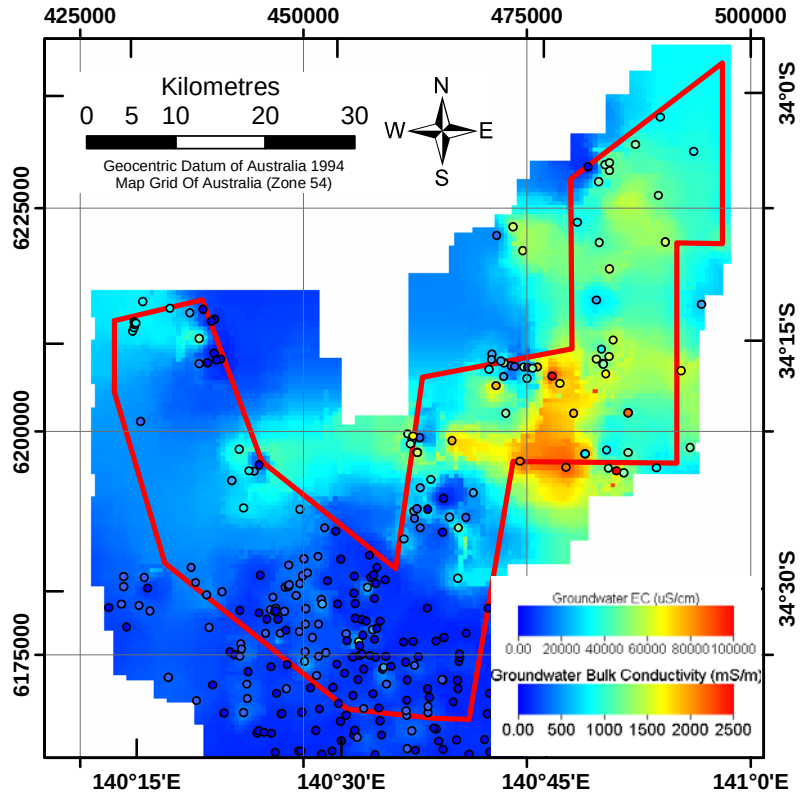

Figure 4.: Groundwater conductivity grided from the same set of boreholes as Figure 3

2. AIRBORNE GEOPHYSICAL DATA

In June 2002 the Bureau of Rural Sciences (on behalf of the South Australian Salt Mapping and Management Support Program (SA-SMMSP) contracted Fugro Airborne Surveys (FAS) to acquire and process airborne electromagnetic (AEM) data over four survey areas. Only the Riverland survey is discussed in this report. RESOLVE data were acquired over a total of 13,145 line kilometres. A summary of the survey parameters is provided in Table 1. The RESOLVE AEM system is a helicopter borne, "rigid" boom, towed bird assembly system.

Table 1. Summary of Riverland RESOLVE HEM survey specifications.

Contracting Organisation	Bureau of Rural Sciences
Client	SA-SMMSP
Contract Supervision Organisation	Geoscience Australia
Survey Company	Fugro Airborne Surveys Pty Ltd
Fugro Airborne Surveys Job Number	1543
Geoscience Australia Project Number	911
Date Flown	26 June 2002 – 26 September 2002
Aircraft	AS-350BA Squirrel, VH-RTV
EM System	RESOLVE
Nominal Terrain Clearance	Helicopter 60 metres Towed bird assembly 30 metres
Total Line Kilometres	11,476 kilometres
Traverse Line Spacing	150/300 metres
Traverse Line Direction	0° - 180° degrees
Tie Line Spacing	4 to 6 kilometres (variable)
Tie Line Direction	90° - 270° degrees

Details of the RESOLVE system are summarised in Table 2 and Table 3. Further details of the data acquisition and processing are provided in the survey Acquisition and Processing Report (Cowey *et al* 2003).

As part of the survey specifications was a requirement to fly a single flight-line repeatedly to monitor system performance during the survey and to better characterise system noise. This line is shown in Figure 1 (RL2), and the resulting data were used (Green and Lane, 2003) to estimate the noise levels shown in Table 3.

Table 2. Summary of RESOLVE AEM system characteristics.

Number of coil sets	6
Navigation	Real time differential GPS mounted on helicopter Ashtech Glonass GG24
Positioning	Post processed GPS mounted on bird Dual-frequency Ashtech Z-Surveyor 1.0 second sample rate
Altimeters	Radar altimeters mounted on helicopter, Sperry RT220 Laser altimeter mounted in bird, Optech G150 0.1 second sample rate
Electromagnetic sampling	6 inphase channels at 0.1 second sample rate 6 quadrature channels at 0.1 second sample rate
Monitor Channels	Horizontal coplanar sferics at 0.1 second sample rate Horizontal coplanar powerline at 0.1 second sample rate Vertical coaxial sferics at 0.1 second sample rate Vertical coaxial powerline at 0.1 second sample rate

Table 3. Summary of RESOLVE coil sets.

Frequency (Hz)	Separation (m)	Orientation	Additive Inphase Noise (Std Dev) Estimate (ppm)	Additive Quadrature Noise (Std Dev) Estimate (ppm)	Multiplicative Inphase Noise (Std Dev) Estimate (%ppm)	Multiplicative Quadrature Noise (Std Dev) Estimate (%ppm)
385	7.86	HCP	2.55	1.5	1.2	1.85
1518	7.86	HCP	4.15	1.9	1.6	2.35
3323	8.99	VCX	2.9	1.5	1.9	2.7
6135	7.86	HCP	5.15	3.2	1.85	2.6
25380	7.86	HCP	8.5	6.65	2.1	2.7
106140	7.86	HCP	13.8	10.4	2.15	2.45

Note: HCP = Horizontal coplanar; VCX = Vertical coaxial

3. OBJECTIVES

The primary objective of the Riverland AEM survey was to map the depth, thickness and conductivity of the Blanchetown Clay in particular. However, a similar understanding of the distribution of other near surface clay rich materials was also important. This is an inversion problem. We must convert in-phase and quadrature measurements of the electromagnetic response into estimates of these geological parameters.

Since geophysical inversion is notoriously ambiguous (many models fit the data within measurement error) it is advisable, wherever possible, to constrain the results of the inversion so that the resultant model parameters are consistent with both the data and *a priori* information obtained from independent sources.

Also, although the RESOLVE system has a very wide bandwidth (100kHz to 400Hz), the system does not sample this frequency range in great detail. It has 6 frequencies in a range of about three decades. A useful rule of thumb is that, to accurately reproduce the full frequency response of a target, you need to sample the spectrum with about five frequencies per decade of range; implying an ideal system should measure at 15 frequencies and not 6.

This under-sampling of the full frequency response means that it is difficult to invert the data to a complete vertical conductivity profile. However, it was clear that, in the Riverland area, it was not

necessary to assume that *any* vertical conductivity profile was possible. In particular there is a great deal of information about the distribution of conductive materials in this area and, because of the well-defined layering and well-characterized water table, it was possible to make some very powerful assumptions about the area before we inverted the data. This, in turn, meant that the restricted number of frequency measurements was no longer such severe constraint on the accuracy of interpretation.

Thus the objectives of this study are to use as much *a priori* information as possible to constrain the inversion of the data from the RESOLVE survey. The inversion will be primarily directed at estimating the depth, thickness and conductivity of the Blanchetown Clay and similar sedimentary materials..

4. METHODS

4.1 Calibration of the Electromagnetic Data

As part of this project the accuracy of the calibration of the RESOLVE HEM data was investigated. This was done by analysis of 32 downhole induction conductivity logs from boreholes located within 60m of HEM observations. The down-hole conductivity information was averaged over 1m intervals and the resulting layered earth model was used, with the observed bird altitude, as input to an EM forward modelling procedure to estimate the expected airborne response.

The forward models were calculated using layered earth forward modelling routines developed at Geoscience Australia. The code is based on the formulation of Wait (1982) for the frequency domain response of vertical and horizontal magnetic dipole sources over a horizontally layered medium. Evaluation of the Hankel transforms was achieved via the filter coefficients derived by Guptasarma and Singh (1997).

Deszcz-Pan *et al*. (1988) discuss methods for calibrating AEM data. They suggest that the observed data is the result of multiple gain and offset distortions of the true data represented by the response predicted by the forward modelling. Thus for observed In-phase and Quadrature data, X_i and X_q with complex representation $X = X_i + jX_q$ and modelled data $M = M_i + jM_q$ then

$$X = Ge^{j\phi}(M + B)$$

Here $Ge^{j\phi}$ is a complex gain and phase correction and $B = B_i + jB_q$ is a complex bias correction. In their formulation ϕ, B_i *and* B_q change on a per-flight basis while G is constant for the whole survey.

In this work we only attempted to correct for the amplitude-scaling factor G. It was felt that further correction on a flight-by-flight basis was both unnecessary and difficult to achieve. The plot, shown in Figure 5, for the highest frequency, illustrates the type of calibration line that was obtained for each frequency. It is clear that the results deviate significantly from the one-to-one line that would imply correct calibration. The most appropriate scaling factors were calculated to be those in Table 4. See Brodie and Green (2003) for a detailed description. All data discussed in this report have been scaled by the factors shown in Table 4.

Table 4. Scaling factors applied to each coil set.

Frequency (Hz)	385.	1518.	3323.	6135.	25380.	106140
Calibration Factor	0.96	1.04	1.11	1.15	1.29	1.23

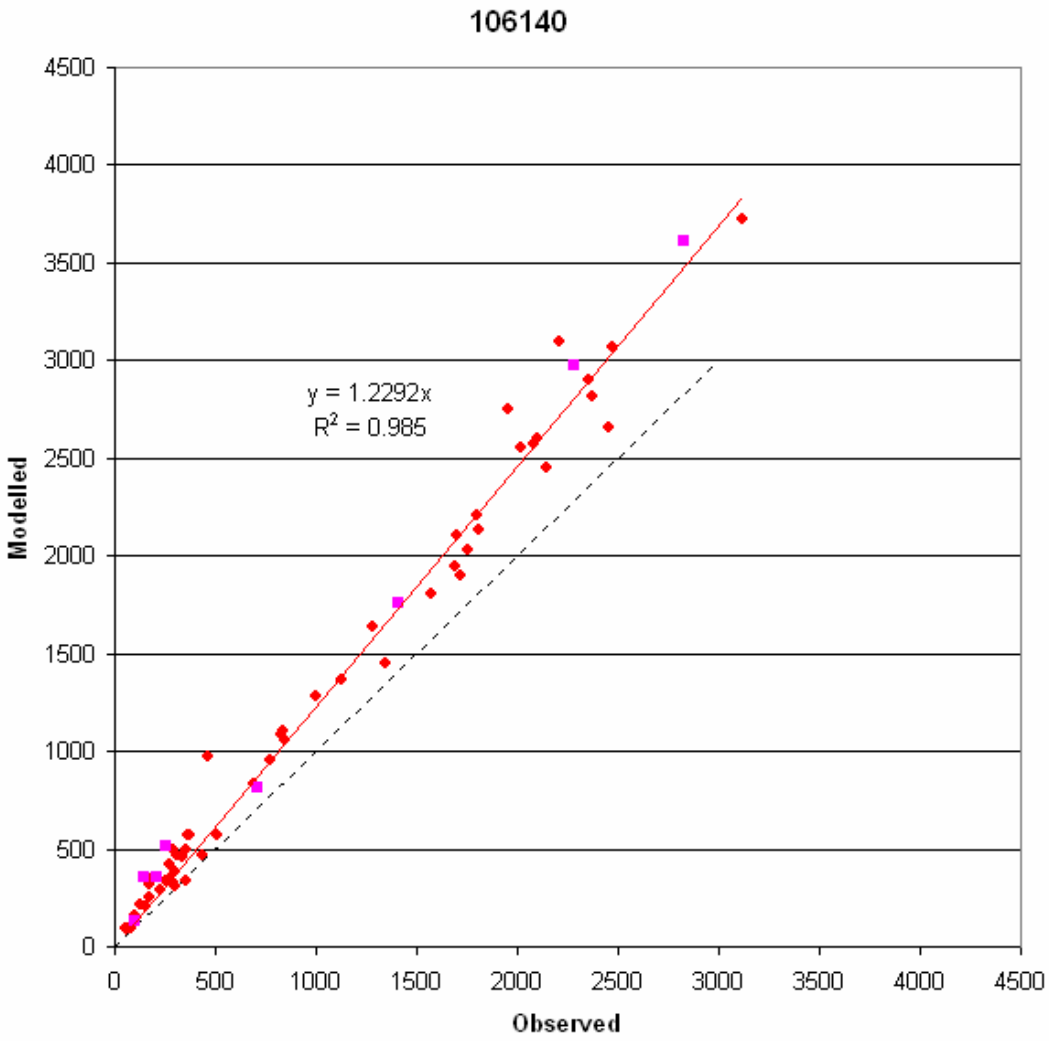

Figure 5.: Calibration plot for the 106140 Hz channel. The X-axis is the observed In-phase and quadrature response (in ppm) and the Y-axis the modelled response for 32 drill holes within 60m of the corresponding airborne sample. The dashed line would be expected if no recalibration were necessary.

4.2 Interpretation of Apparent Conductivity Images

For each frequency, FAS supplied Apparent Conductivity and Apparent Depth inversions. These are produced by a simple inversion process that returns the conductivity and depth of the homogeneous half-space that would cause the AEM system to produce the observed responses at each frequency (Fraser, 1978).

If the ground had no vertical layering, i.e. had the same conductivity at all depths, then this inversion would be correct and all frequencies would produce the same result. Even though this is rarely the case, Apparent Conductivity images can be very useful intermediate products for interpretation. Their most useful attribute is that they no longer show much of the helicopter altitude variability that is inherent in the raw In-phase and Quadrature data.

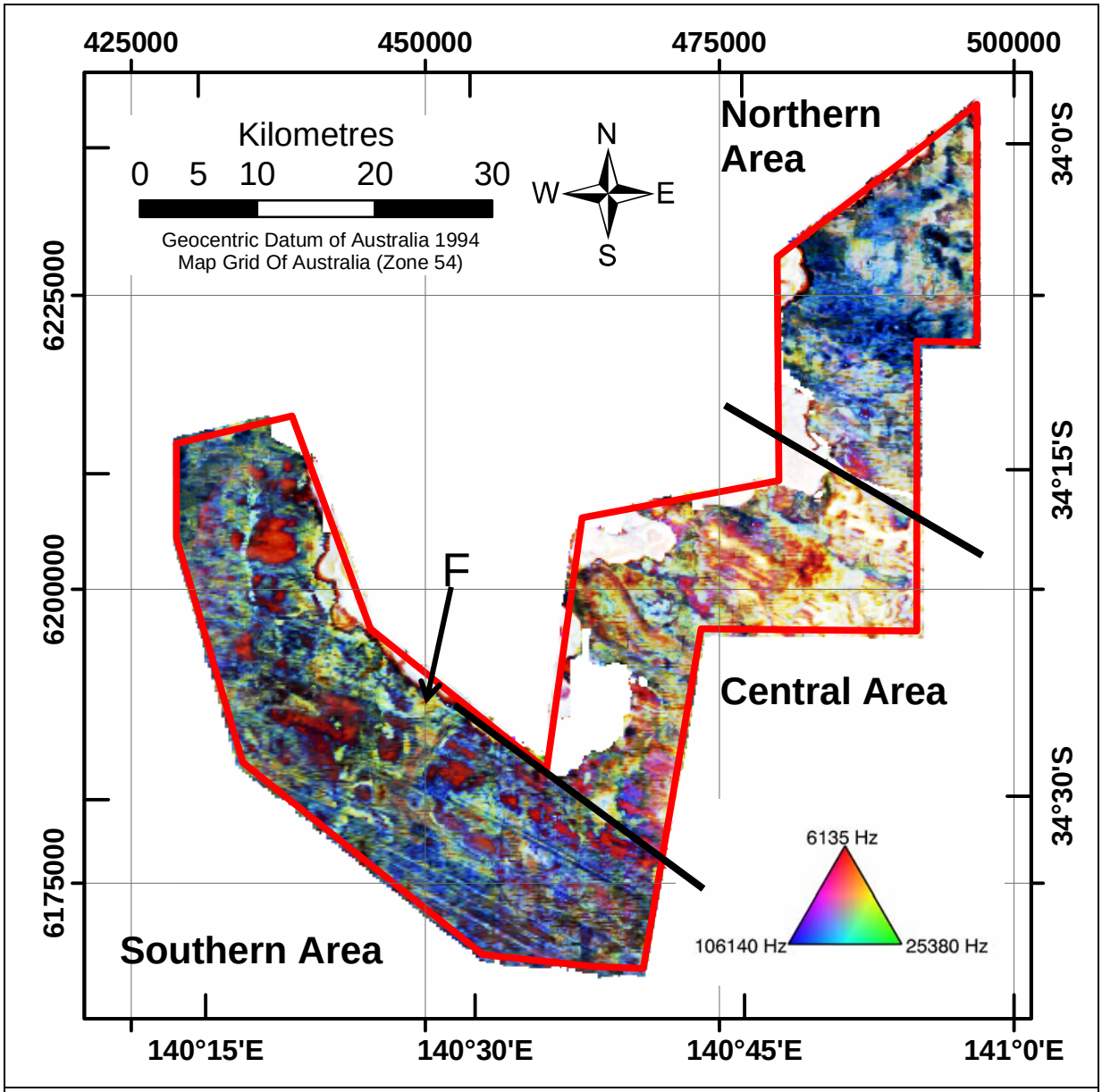

Figure 6.: RGB composite of the apparent conductivity in the 6135, 25380 and 106140 Hz channels. The data have been logarithmically stretched before display.

In this project we have found that colour composite images of the Apparent Conductivity data have been very useful in the preliminary stages of interpretation. While it is difficult to interpret these products in terms of accurate thicknesses and conductivities they do provide high quality images that can be used to locate interesting areas for further study. Figures 6 and 7 show the RGB composites for the highest and lowest frequencies respectively.

Figure 6 displays almost all the shallow variability in the data. The patterns in the image are caused by the variable distribution, thickness and conductivity of near-surface clay. Based on this data, the study area divides naturally into three distinct regions. The Southern Area to the south and west of Loxton, the Central Area between Loxton and the Stuart Highway and the and the Northern Area north of the Stuart Highway. The flood plain of the River Murray, white on all apparent conductivity products, is really separate from these discussions.

In the Southern Area the NW-SE strandline pattern is obvious and tends to dominate and control the clay distribution. Thick, conductive clays are shown in white and yellow, thinner clays show in blue. Where there is higher conductivity at depth (probably at the water table) and the clay is absent the

image is a dark red. This colouration an also be seen in places where the clay, although not absent, is very thin. These red areas are invariably local topographic lows. Although the strandline pattern controls much of the clay distribution in this area there are some very obvious cross-cutting features, most notably the (possibly fluvial?) feature at F in Figure 6.

The Central Area is generally topographically lower, has thicker clays and their distribution is no longer controlled by the stand-line pattern. This area is also complicated by the presence of shallow conductive groundwater that increases the overall brightness of the image in this area.

The Northern Area is dominated by the high (85 m) ridge and has some clay which, except perhaps in the southernmost part, is not controlled by the strandline pattern.

Figure 7 displays conductivity structure that is deeper than that shown in Figure 6. However, because the deeper features are masked where there are thicker clays near the surface, this image shows a mixture of deep and shallow features. Where there is little or no near-surface clay the system appears to be "seeing through" to the water table and the brightness reflects this deep conductivity. These areas are whitish, some brighter than others. The darker areas are where there is appreciable near-surface clay, which at these low frequencies, gives a mixed apparent conductivity signature. In general, the thicker the clay, the more blue and brighter the image.

4.3 Inversion Procedure

The choice of the geological model to be used for the inversion is critical to the success of the project. If we choose to invert for a geology that is substantially different from the actual situation, we can expect the results to be very unreliable. In this work we have made an important assumption about the geology in the survey area. When we invert the data at a particular location we assume that the earth in the vicinity of the HEM sensor is composed of a small number (~5) of discrete horizontal layers of infinite lateral extent. Each of these layers is assumed to have constant conductivity and thickness.

Obviously, this one-dimensional, "layer-cake" model is only an approximation to the real world. For it to be a reasonable approximation, the geology must vary slowly as a function of position and the geological units must be relatively uniform and without sudden changes in conductivity in any direction. When we say "slowly" we refer to the scale of the measurement system. For lateral variability, this scale is dominantly determined by the altitude of the sensor (30 m). Thus we would like the geology to be a good approximation to a 1-D layer-cake over distances two to three times this altitude, typically an area of one hectare.

This is probably a reasonable approximation over much of the survey area but there are certainly places, over sharp geological boundaries particularly, where it breaks down. In these places the results of the inversion must be treated with suspicion. To correctly model these situations would require a much more sophisticated, computer-intensive model.

Based our knowledge of the geological section and its history we initially expected to have a simple four-layer geophysical model comprising resistive sands over the more conductive Blanchetown Clay overlying the Loxton-Parilla Sands which are resistive when dry and conductive below the water table.

Given a simple 1-D model like this we must also be able to legitimately impose upon it our *a priori* knowledge about the area. Such knowledge can be quite specific and provide strong constraints. For example, if we are sure that the water table is at 26 m depth, we can force the thickness of all the layers above the water table to add to 26m. We can think of this as a "hard" constraint.

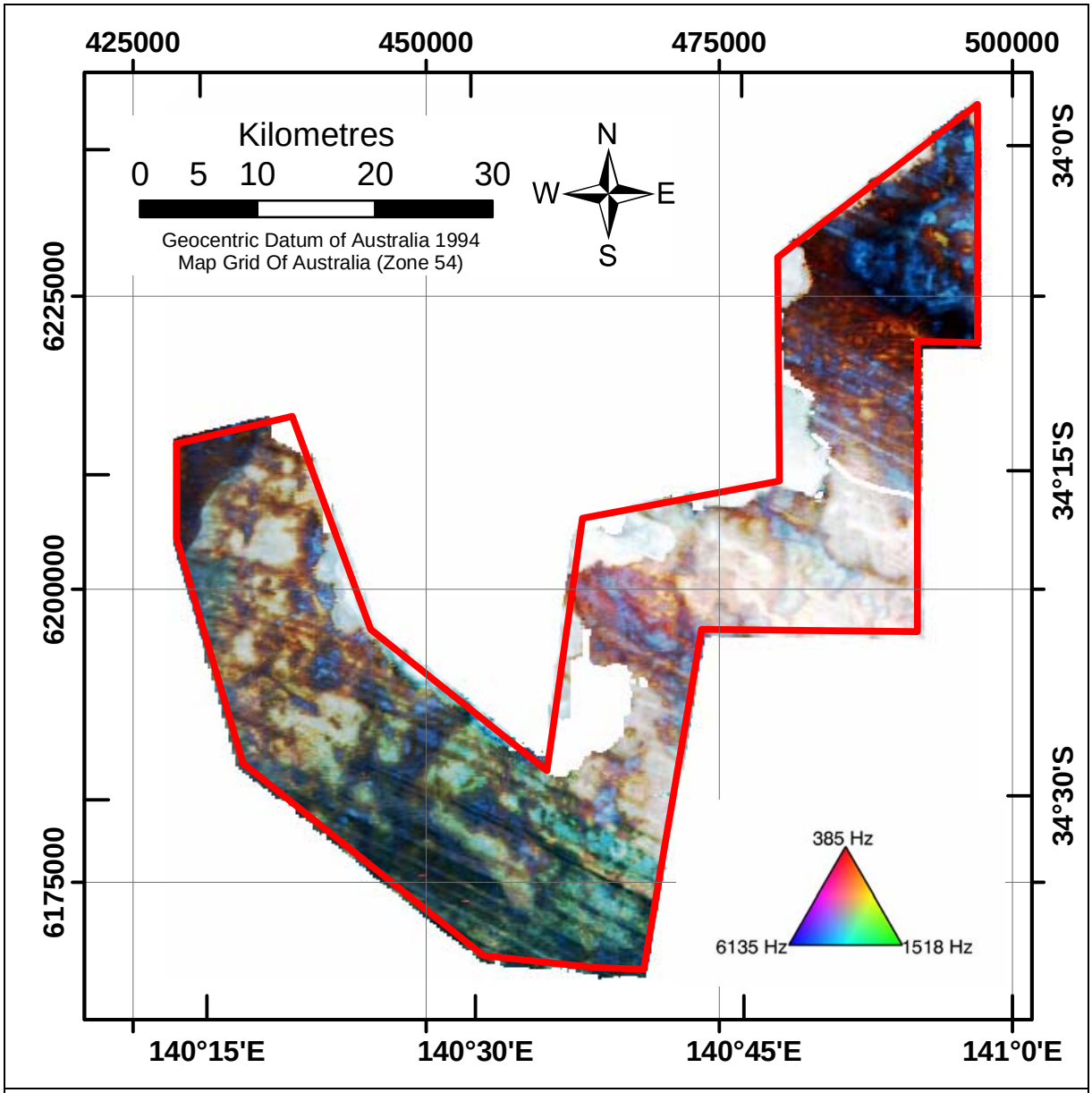

Figure 7. RGB composite of the apparent conductivity in the 385, 1518, 3323 Hz channels respectively. The data have been logarithmically stretched before display.

Alternatively, if we expect the conductivity of the saturated aquifer to be in the general vicinity of 250 mS/m we can "suggest" to the inversion procedure that this would be a good place to start without forcing it to adopt this value. This can be thought of as a "soft" constraint. Most types of constraints can be adjusted to be hard, soft or somewhere between depending on our level of confidence in them.

The main constraints available in this area relate to the saline groundwater. Except where fresh water from irrigation complicates the problem, it is clear that there will be a major conductivity contrast at the water table and that it is logical to define a layer boundary at this level.

Further, in the absence of clay-rich lithologies, it is reasonable to expect that the conductivity below the water table to be determined by the conductivity of the groundwater and the porosity. As we have the spatial variation in the groundwater conductivity we needed a way to convert from groundwater conductivity to bulk conductivity. To do this we used down-hole induction logs that were near to where groundwater conductivity observations were available, to calibrate between the bulk conductivity (from the logs) and the groundwater conductivity.

The resulting calibration line is shown in Figure 8. Thus, to convert groundwater conductivity (in mS/m) to bulk conductivity we have multiplied by 0.25.

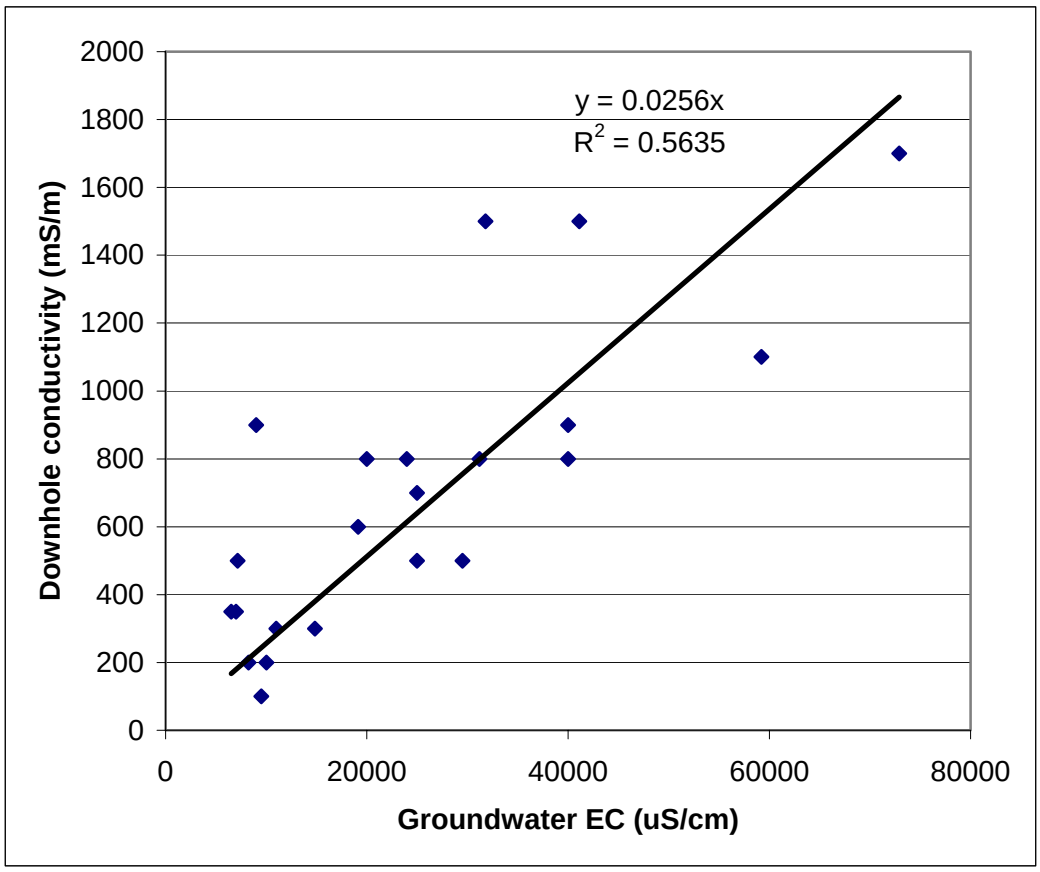

Figure 8.: The relationship between groundwater conductivity and observed bore conductivities used to convert to bulk conductivity for layers below the water table.

In assuming that this calibration curve applies all over the survey area we are, of course, making a considerable simplification. This might be justified for the Loxton/Parilla Sands and the limestone of the Murray Group but where the marine clays of the Bookpurnong Beds are involved some modification could be expected. Nevertheless the Bookpurnong Beds are usually quite thin (< 10m) and the conductivity could reasonably be expected to revert to the predicted value in the Murray Group formations below.

This concern was confirmed on examining induction logs that showed that although the deeper conductivity was usually about the value expected on the basis of the groundwater, there were often situations where there was a bulge of higher conductivity close to the position of the water table. A typical example is shown for hole LH041G (figure 9). This hole shows a marked increase in conductivity just below the water table. Below the bulge, the conductivity drops back to a value (~300 mS/m) consistent with the groundwater conductivity. In contrast, PYP5, a hole quite close to LH041G, did not show a similar bulge. This, and the fact that these holes (and others like them) were located in areas that showed quite different responses on the low frequency Apparent Conductivity image led to the conclusion that there was a factor, other than the groundwater variability, that was at work in determining the spatial variability of bulk conductivity near the water table.

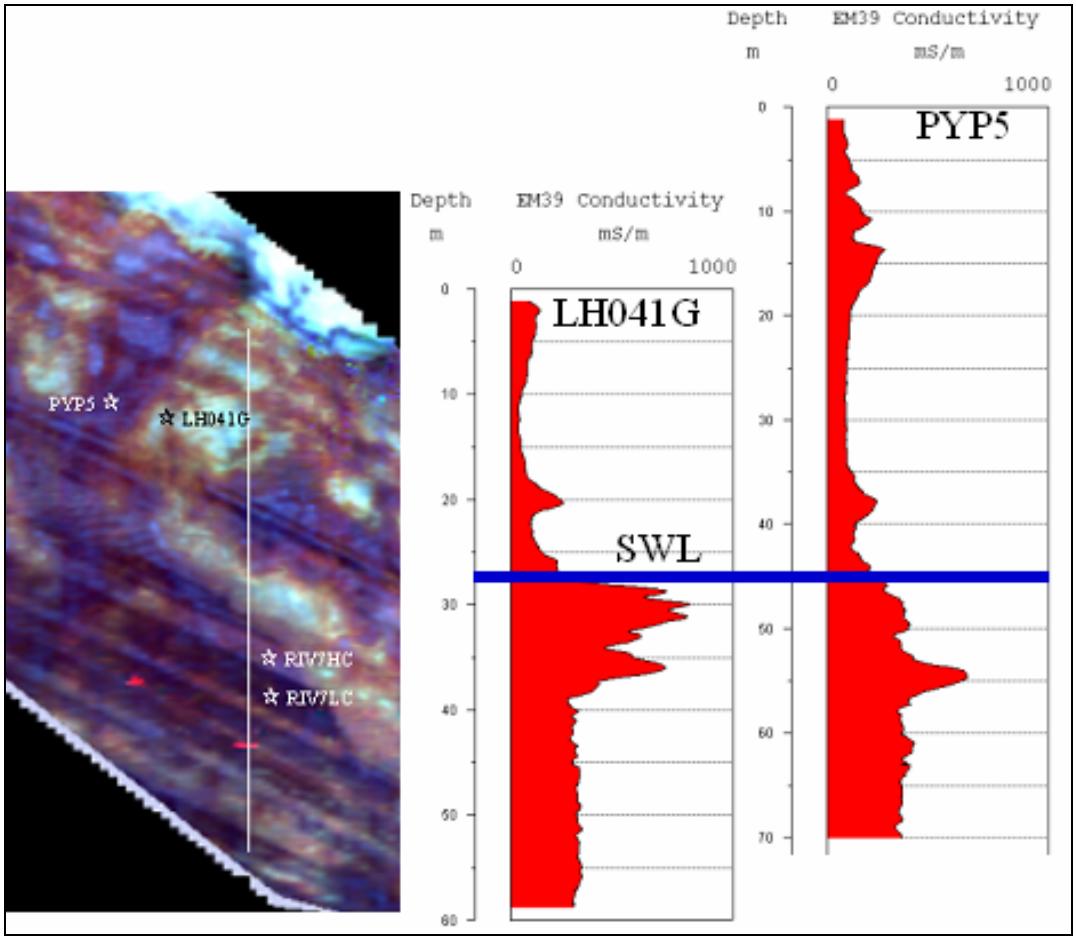

Figure 9:. Induction logs for adjacent drill holes that show differing conductivity patterns near the water table. Location is on the low frequency Apparent Conductivity image.

To accommodate this factor we modified the geophysical model (Table 5) to include an extra layer, with thickness fixed at 10m, just below the water table. The "basement" below this layer was then treated as a layer with conductivity typical of the groundwater.

Table 5. Initial assumptions about the conductivity structure in the Riverland Area.

Layer 1	Recent Sands	Non-conductive (~30 mS/m) Thickness variable between a few meters and 10m in isolated areas
Layer 2	Blanchetown Clay	Conductive (100–400 mS/m). Thickness: Usually a few meters, up to 10m in isolated areas. Absent in eroded areas.
Layer 3	Loxton-Parillia Sands above the water table	Non-conductive (~50 mS/m) Thickness: Variable depending on the water table. Typically 15-30 m.
Standing Water Level		
Layer 4	Conductivity Bulge, perhaps associated with the fine grained sediments of the lower Loxton and/or the Bookpurnong Beds	Conductivity variable upwards from that of layer 5, Thickness fixed at 10m.
Layer 5	Saturated Loxton-Parillia Sand and/or Murray Group limestone below the water table	Conductive as determined by the porosity and the conductivity of the groundwater. Assumed to extend infinitely downwards.

This five-layer model has nine parameters that enable the AEM response to be calculated. They are the thickness and conductivity of the first four layers and the conductivity of the fifth. Geophysical inversion is the process of adjusting these parameters, within the constraints imposed by our *a priori* knowledge, until we can reproduce the observed response. The inversion procedure used here follows Menke (1989). In this section we review the method in a qualitative manner and Appendix 1 gives the mathematical details

This adjustment is an iterative process that starts from initial parameter values and alters the parameters in small steps so as to reduce the magnitude of the *objective function* Φ. The formula below, while not mathematically rigorous, attempts to convey the nature of this function.

$$\Phi = \sum_{i=1}^{12}\left(\frac{d_i - L_i(m_1 \ldots m_9)}{(noise)_i}\right)^2 + \sum_{j=1}^{9}\left(\frac{m_j - \hat{m}_j}{(spread)_j}\right)^2$$

Here d_i, $i=1..12$ are observed AEM data values and m_j, $j=1..9$ are the current set of model parameters. $L_i(m_1 \ldots m_9)$ is the modelled response in the i^{th} AEM channel. This forward model is the same as the one used for the data calibration described in Section 2.1. Φ is composed of two summations, one over the data misfits and the other over the model misfits.

Considering data misfit first. If the current model parameters match the correct geology then each $L_i(m_1 \ldots m_9)$ will be close to the corresponding d_i value and terms in the numerator of the left-hand summation will be small. These differences are normalized by the noise in each channel in order to balance the contribution of each channel to the total. Thus a noisy channel will be down-weighted and a relatively noise-free channel given more weight. The noise values were computed as the sum of the additive and multiplicative components given in Table 3.

In the right-hand summation, the $\hat{m}_j$, $j = 1 \ldots 9$ are a reference set of model parameters selected on the basis of our *a priori* knowledge of the area. When the current model parameters differ from the reference set, Φ increases, making it less likely that we will choose this set of parameters. The difference between each parameter and its reference value is normalized by a measure of our confidence in the reference value, here called the "spread". If we wish to force the inversion to adopt a particular value we can make this quantity very small. The effect of the difference between the current value and the reference value will be magnified to such an extent that the reference value will be accepted irrespective of the effect on the data misfit.

On the other hand, if we have no confidence in a reference value we can make the corresponding spread very large and it will hardly influence the value of Φ at all. It should be noted that, even if this is the case, it does not mean that the reference value will not influence the final result. This is because the reference values are also used as the starting values for the iterations that seek to reduce the value of Φ. When, as in this case, the forward model that calculates the $L_i(m_1 \ldots m_9)$ is non-linear, the final result of the inversion can depend on the starting values for the model parameters.

The reference values and their spreads allow us to constrain each model parameter to an approximate range but a further refinement is necessary to implement our constraint that the thickness of the layers above the water table should add to the known water table depth. This constraint was implemented by introducing the water depth as an extra, 13^{th} data value and including an extra equation for $L_{13}(m_1 \ldots m_9)$ that models the depth as the thickness of the first three layers. The "noise" normalization term for this data value was then given an extremely low value thus forcing the model parameters to match the observed water depth.

Using the logarithms of the conductivity (σ) and thickness (t) as the model parameters instead of the normal values further stabilized the inversion. This transformation enforces a positivity constraint and

also allowed us to set a minimum value for the clay conductivity. Because the model parameters are of the form $\log_{10}(\sigma)$ or $\log_{10}(t)$ the numerators of the second summation in Φ are terms of the form $\log_{10}(\sigma/\hat{\sigma})$ or $\log_{10}(t/\hat{t})$.

The spread for each parameter is then the log of the fractional acceptable change in the ratio of the conductivities or thicknesses. Thus a value of 1 is a very loose constraint that suggests that a factor of 10 (1000%) between the current and reference parameter is acceptable. A value of 0.3 corresponds to a factor of ~200% and 0.05 a factor of ~10%.

Table 6.: Summary of inversion parameters

Parameter name	**Symbol**	**Inverted quantity**	**Spread Factor**	**Reference and Initial Values**
Recent Sands: Conductivity	σ_{s1}	$\log_{10}(\sigma_{s1})$	0.05	0.030 S/m
Blanchetown Clay: Conductivity	σ_c	$\log_{10}(\sigma_c\text{-}0.1)$	0.10	0.240 S/m
Lower sand (dry) Conductivity	σ_{ls}	$\log_{10}(\sigma_{ls})$	0.05	0.065 S/m
"Bulge" Conductivity	σ_b	$\log_{10}(\sigma_b)$	0.25	$0.25\sigma_w$(x,y) S/m
"Basement" Conductivity	σ_w	$\log_{10}(\sigma_w)$	0.05	$0.25\sigma_w(x,y)$ S/m
Recent sand thickness	t_{s1}	$\log_{10}(t_{s1})$	1.0	3.0 m
Blanchetown Clay thickness	t_c	$\log_{10}(t_c)$	1.0	3.0 m
Lower sand thickness	t_{ls}	$\log_{10}(t_{ls})$	1.0	$d_{gw}(x,y) - t_{s1} - t_{bc}$ m
"Bulge" thickness	t_b	$\log_{10}(t_b)$	0.05	10.0 m
$\sigma_w(x,y)$ = Groundwater conductivity as shown in figure 4 $d_{gw}(x,y)$ = Depth to groundwater, determined as the difference between topography (figure 2) and groundwater elevation (figure 3) Hard Constraint: $t_{s1} + t_c + t_{ls} = d_{gw}(x,y)$ All inversion were performed in units of Siemens/metre for conductivities or metres for thicknesses.				

These parameters were established by an extensive set of tests where individual samples and selected flight-lines were inverted and evaluated by comparing the results with known and expected clay distributions. Once established every fifth sample from the whole survey was inverted. This sampling density, approximately one sample every 15m, was adjudged sufficiently dense for the purposes of the project.

At this sampling density 727,496 inversions were required to process the whole survey. This would have taken an impossibly long time running on one PC. To overcome this problem, a master-slave distributed processing application was developed in which a master computer assigned small packets of work to multiple slave computers across the network to be run as low priority (background) tasks. Upon completion of a packet of work by each slave the results were sent back to the master computer for storage in a merged file. In this way 58 PC's were used to complete the inversion of the full dataset in approximately 26 hours.

After merging of the data all conductivity and thickness estimates were filtered with a 5 point median filter (length ~ 75 m) to produce the final parameter set. These results can be displayed either as sections (see Figure 10) or as plan format images.

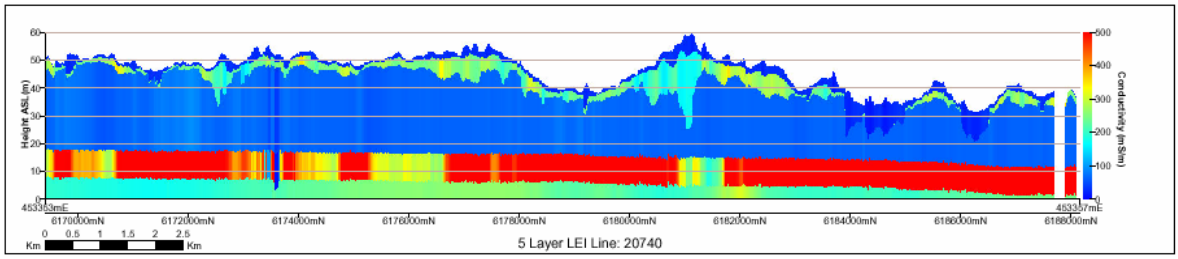

Figure 10.: Stitched section of inversion results for the line plotted on the image in Figure 9.

In some areas where the Blanchetown clay appears to be absent, the inversions accommodated the observed response by predicting a non-negligible thickness of low conductivity clay at significant depth (most often 10m or greater) rather than predicting a very thin shallow clay at as would have been ideal. These artefacts were easy to identify in conductivity sections and a simple rule could be applied to the median filtered dataset to eliminate them. The rule is defined as follows: If the elevation of the top of the clay was below 30m and the thickness of the upper sand layer was greater than 5m, then the thickness of the clay layer was set to 0.01m and the thickness of the lower sand layer was set to the sum of the thickness of the clay and lower sand layers.

This rule was not applied in the zone east of 469,000mE or south of 6,213,000mN because in this zone there are real clay deposits whose elevation is less than 30m underlying substantial sand cover. In parts of this zone the surface elevation is low

Post-processed versions of the Blanchetown Clay thickness and elevation of its base were produced at this point as products to illustrate the distribution of significantly thick clay over the survey area. The clay thickness was set to undefined (ie. nonexistent) if its thickness was less than 0.25m. This had the effect of removing the clay where it was poorly resolved (because of thinness).

The elevation of the base of the clay was calculated by subtracting the sum of the upper sand and clay thicknesses from the surface elevation. Again these data were set to undefined if the thickness was set to undefined as explained above. Further points were set to undefined if the surface elevation was below 16m. At these points low lying points of the landscape the clay is not expected to be present or is difficult to resolve with the observed data because the saline watertable is very close to the surface.

The samples from the polygon labelled G on Figure 2 were subject to different processing to the rest of the survey area. This is clearly an area of very thick clays and the actual distribution of conductivities is so different from the rest of the area it could not be processed satisfactorily without changing the reference and initial parameters. In this area the reference and initial conductivities were elevated to the values shown in Table 7 based on observations of nearby down-hole logs the intersected the Blanchetown Clay. Spread factors were not changed for this area. No attempt was made at smoothly matching the inversions in side the area G to those outside it. The coordinates of the polygon are provided in Appendix 3.

Table 7.: Summary of inversion parameters for the area labelled G on Figure 2.

Parameter name	Symbol	Inverted quantity	Spread Factor	Reference and Initial Values
Blanchetown Clay: Conductivity	σ_c	$\log_{10}(\sigma_c\text{-}0.1)$	0.10	1.000 S/m
"Bulge" Conductivity	σ_b	$\log_{10}(\sigma_b)$	0.25	1.500 S/m
"Basement" Conductivity	σ_w	$\log_{10}(\sigma_w)$	0.05	1.500 S/m

5 RESULTS

The 5-layer inversion procedure used here has a nominal nine parameters; four thicknesses and five conductivities. However because the thickness of the "Bulge" layer was fixed at 10m it need not be considered further. Also, because the conductivity of the lowest layer was held relatively tightly to the value determined by the groundwater conductivity, this particular parameter is merely a copy of the constraint data and would appear as that shown in Figure 4. Images of the remaining parameters are shown in the following sections.

5.1 Parameter Images

In most of the survey area the pattern of the Recent sand dunes dominates the thickness of the first layer (Figure 11(a)).

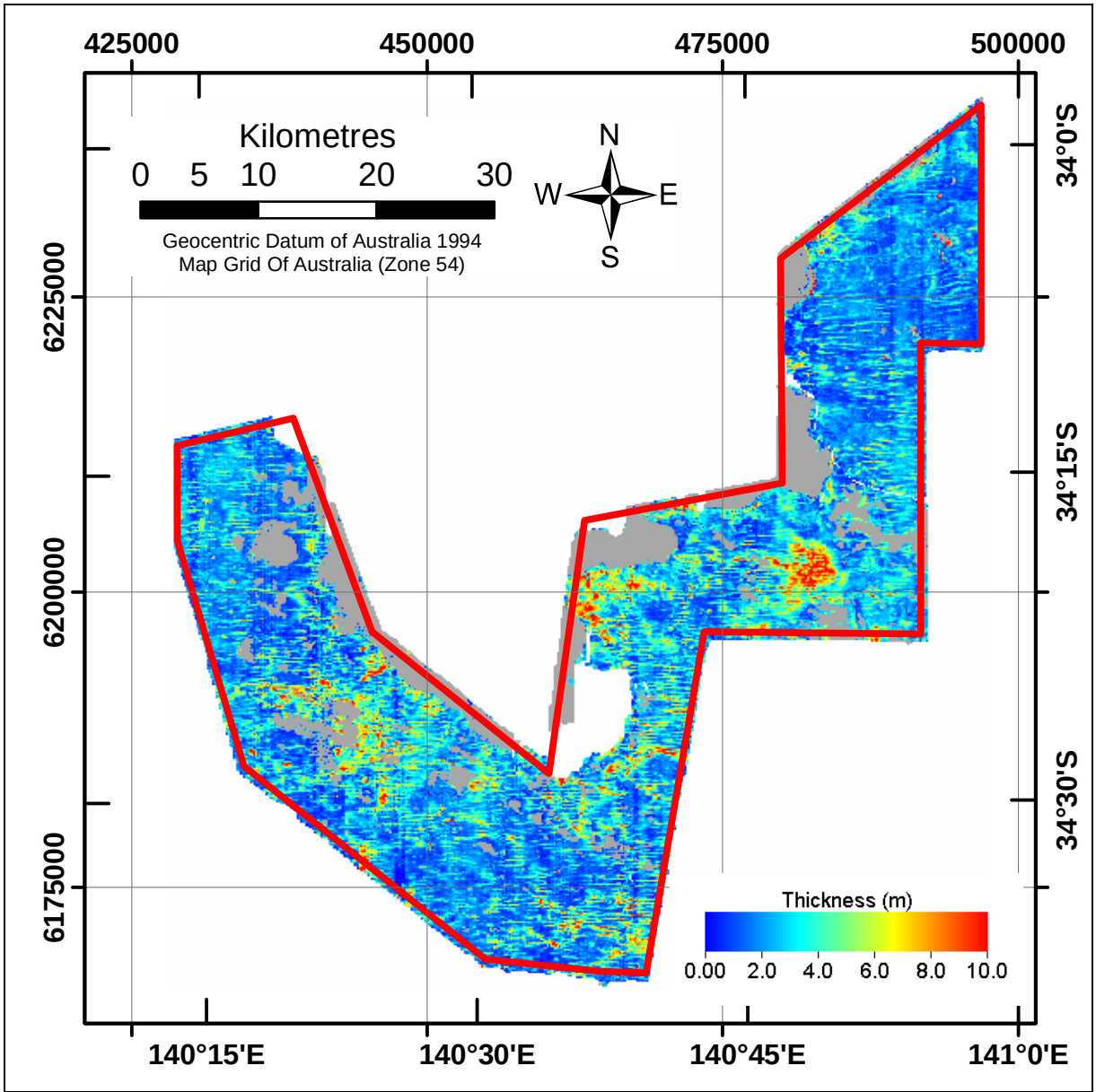

Figure 11(a). Thickness of the first (Recent sand) layer.

The grey areas are locations where the model used for the inversion is inappropriate. These occur on the Murray floodplain and where, as discussed above, the inversion detected less than 0.25m of clay. (Note, this is a function of the inversion model and does not reflect the presence of clay rich sediments known to occur on the flood plain). There are thicker, up to 10m, localized accumulations of sand that

are unrelated to this pattern. The most obvious of these occurs over area G (Figure 3) and may be the result of the different processing that was applied in there.
The complex patterns of clay thickness (Figure 11(b)) clearly indicate that the clay distribution has been controlled by a number of geomorphic processes. In the Southern Area clays have been retained on the high ground and eroded from to low points in the landscape. Generally, their distribution is controlled by the strandline pattern but there are also obvious cross-cutting features which suggest that clay rich materials may have been re-distributed and concentrated in certain parts of the landscape by either fluvial and/or aeolian processes..

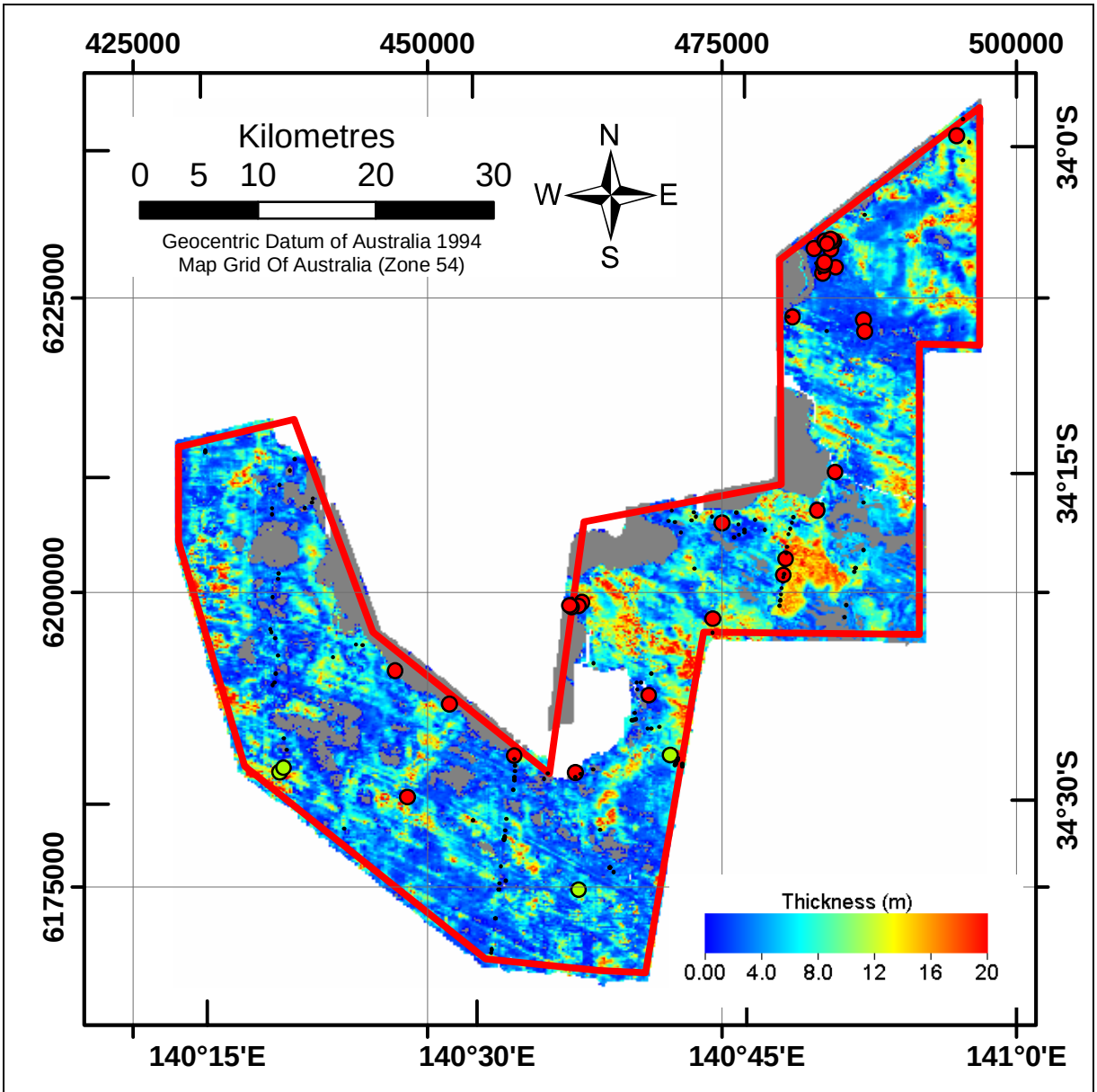

Figure 11(b). Thickness of the second (clay) layer. The red and green spots locate drill holes with induction logs that are a poor match with inversion results.

In the Central Area, although there is some evidence of strandline control, the clay distribution is much more complex. More work is required to understand what is going on in this area.

In the lower, southern part of the Northern Area the clay distribution is controlled by the strandlines. However to the north, where the clay is above the elevation of Lake Bungunnia (~60 m), the pattern is irregular. Also, on the SW facing slope of the ridge that dominates the area, there is almost no clay.

It is likely that this clay distribution is the result from deflation off the old lakebed and the windward side of the ridge and subsequent re-deposition on the lee side of the ridge. The prevailing wind direction is from the South West.

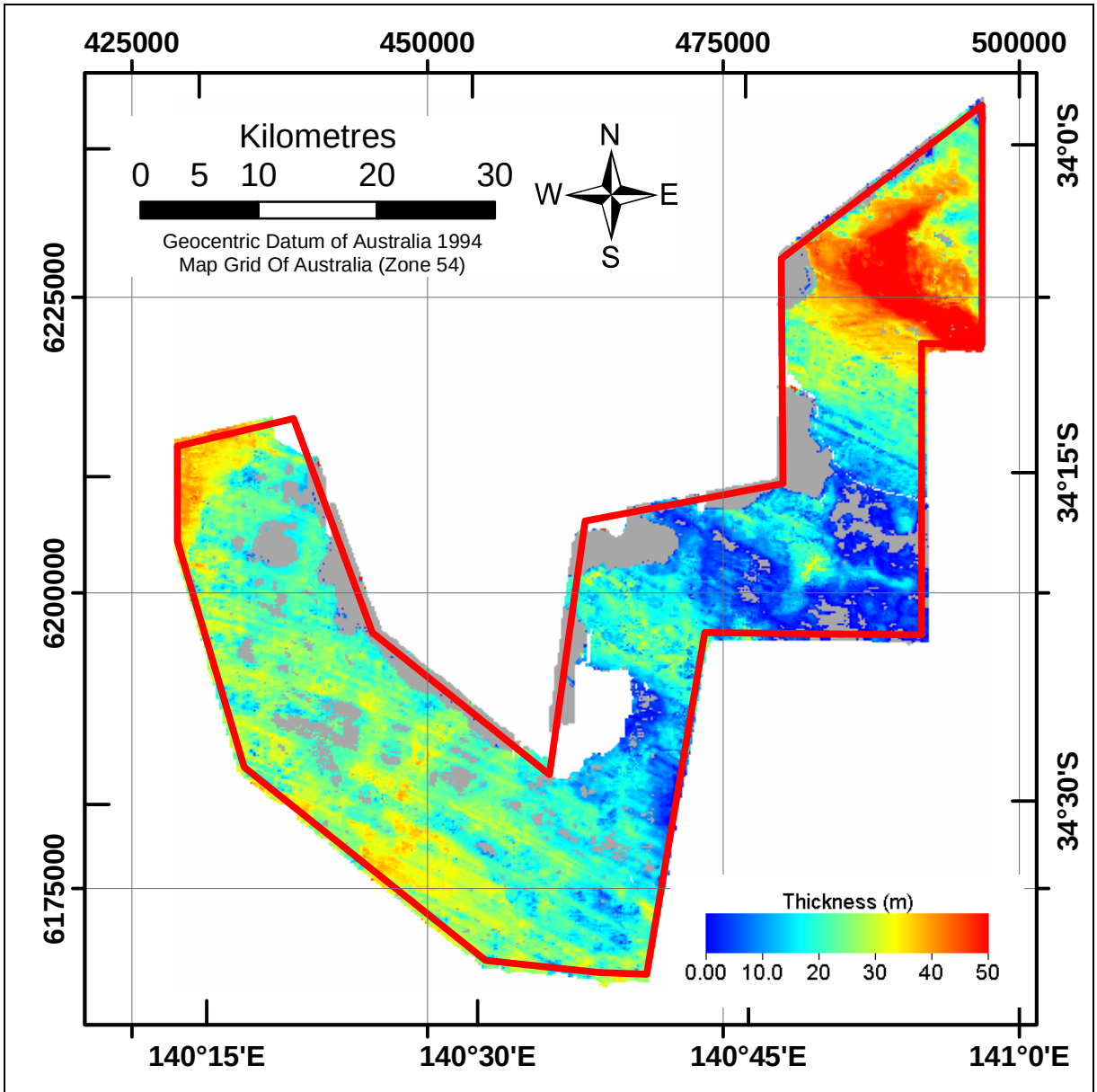

Figure 11(c).: Thickness of the third (lower dry sand) layer.

The thickness of the third layer (Figure 11(c)) is effectively the distance the water table is below the clay. Because the water elevation varies quite slowly the image expresses the detail of the pre-Bungunnia topography quite well.

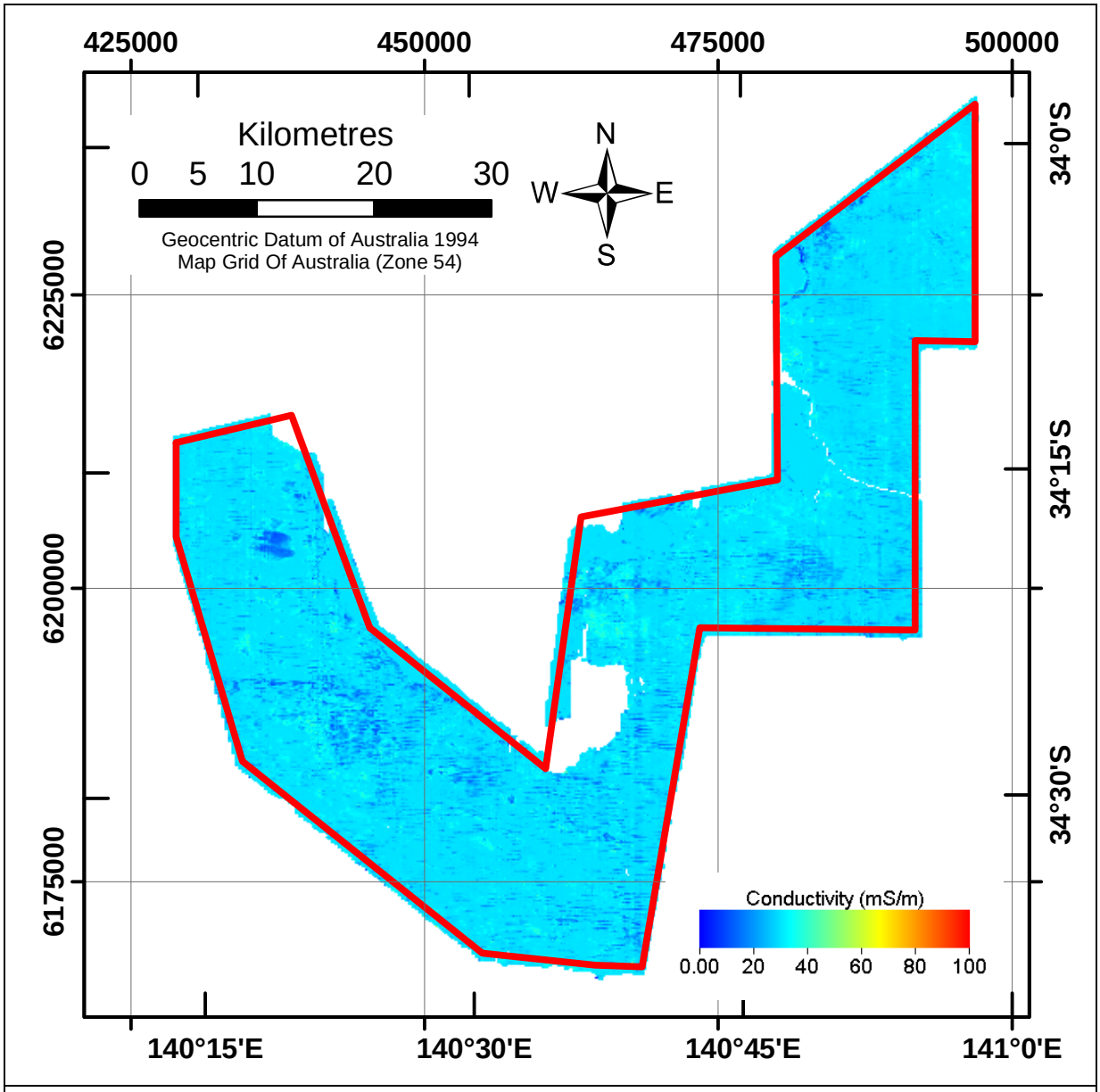

Figure 12(a).: Conductivity of the first layer.

The conductivity of the first layer (Figure 12(a)) is very uniform and low. This is because the inversion has constrained it to be so. As a result of the more relaxed inversion constraints, the clay conductivity (Figure 12(b)) shows a wider range of conductivities. There are no values less than 100 mS/m because the constraining procedure used $\log_{10}(\sigma_c\text{-}100)$ as the inversion parameter to force a minimum value. This means that, in areas where the second layer was more resistive than 100 mS/m it was forced to be thinner.

The conductivity of the third layer was constrained quite rigidly and, as result the corresponding image (Figure 12(c)) is very uniform.

The conductivity of the "bulge" layer (Figure 12(d)) is perhaps the most unexpected and intriguing result of the inversion. The patterns in each of the three areas (Southern, Central and Northern) are quite different in character and will be dealt with in turn.

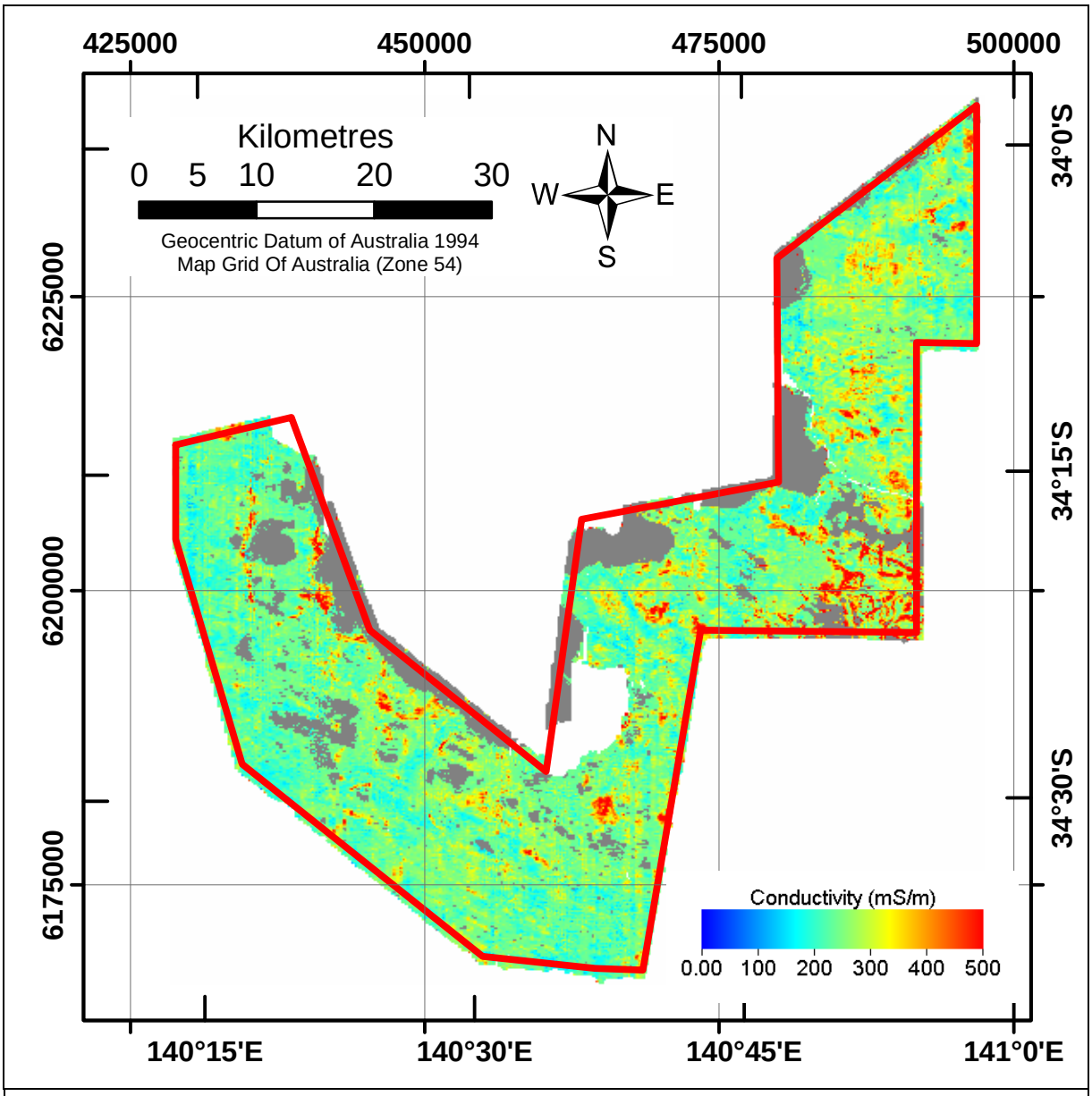

Figure 12(b).: Conductivity of the second (clay) layer

In the Southern Area, two patterns are evident. The SE part of the area is dominated by a strandline pattern while the NW is more conductive and does not show the strandline pattern.
We know from drill hole information, that the Bookpurnong Beds, a late Miocene-Early Pliocene marine clay immediately below the Loxton/Parilla Sands, comes progressively closer to the surface as we move NW. It is likely that the more conductive material showing in this image is associated with situations where the water table is below the strandline-patterned Loxton/Parilla Sands and in the conductive clays of the Bookpurnong Beds.

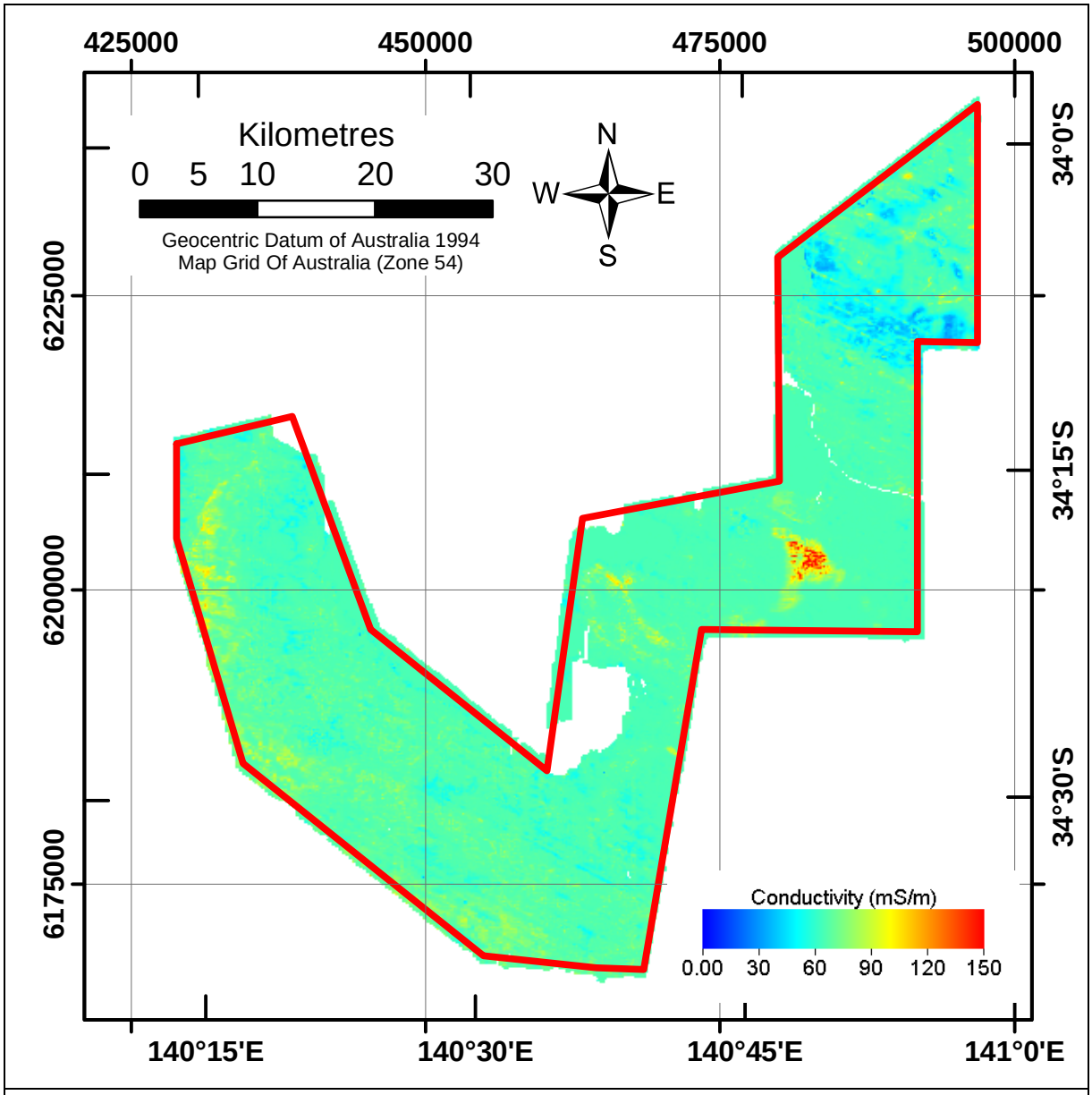

Figure 12(c).: Conductivity of the third layer

The conductivity of the "bulge" layer (Figure 12(d)) is perhaps the most unexpected and intriguing result of the inversion. The patterns in each of the three areas (Southern, Central and Northern) are quite different in character and will be dealt with in turn.

In the Southern Area, two patterns are evident. The SE part of the area is dominated by a strandline pattern while the NW is more conductive and does not show the strandline pattern. We know from drill hole information, that the Bookpurnong Beds, a late Miocene-Early Pliocene marine clay immediately below the Loxton/Parilla Sands, comes progressively closer to the surface as we move NW. It is likely that the more conductive material showing in this image is associated with situations where the water table is below the strandline-patterned Loxton/Parilla Sands and in the conductive clays of the Bookpurnong Beds.

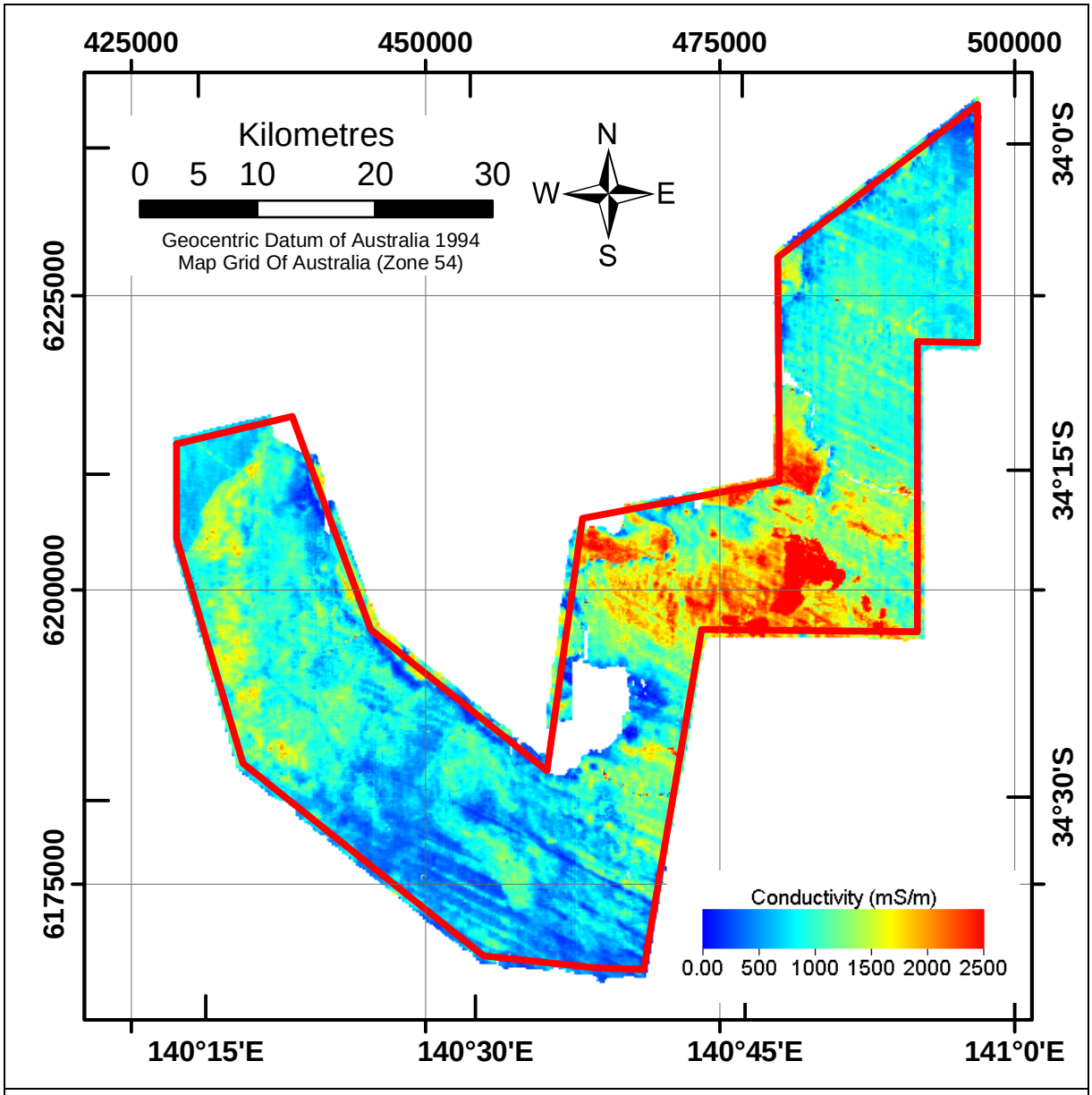

Figure 12(d).: Conductivity of the fourth (bulge) layer.

Further, in the extreme NW corner of the survey the conductive Bookpurnong pattern disappears at a very sharp boundary with a more resistive, spatially uniform pattern. Here it is likely that Bookpurnong disappears from the section and the water table is in more resistive limestone.

The cause of the observed conductivity structure at depth in the in the SW part of the Southern Area is not clear. It could be due to a systematic variation in the porosity of Loxton/Parilla Sands where they are intersected by the water table. If this is true it could have important implications for hydrological models of the area. However, the deep strandline pattern could also be due to strandline-correlated variability in the elevation of the contact between the Bookpurnong Beds and the Loxton/Parilla sands. All through this area the water table is within a few meters of this contact and it would not be unexpected for the contact to show the same strandline patterns.

In the Central Area the conductivity is dominated by the saline groundwater coming from the east and the effect of the fresh water introduced by the irrigation around Loxton. In these more resistive areas around Loxton the strandline pattern disappears. It is difficult to know if this is due to the effect of the irrigation water (which is most likely), or more complex variation in the subsurface stratigraphy.

In the Northern Area a simple strandline pattern again dominates the deeper conductivity.

5.2 Derived Parameters

One of the most instructive data sets that can be derived from the inversion results is the elevation of the base of the clay layer (Figure 13). Except were the clay is absent or redistributed, the images show the palaeo-topography of the Pliocene strandline pattern post deposition and just before the formation of Lake Bungunnia.

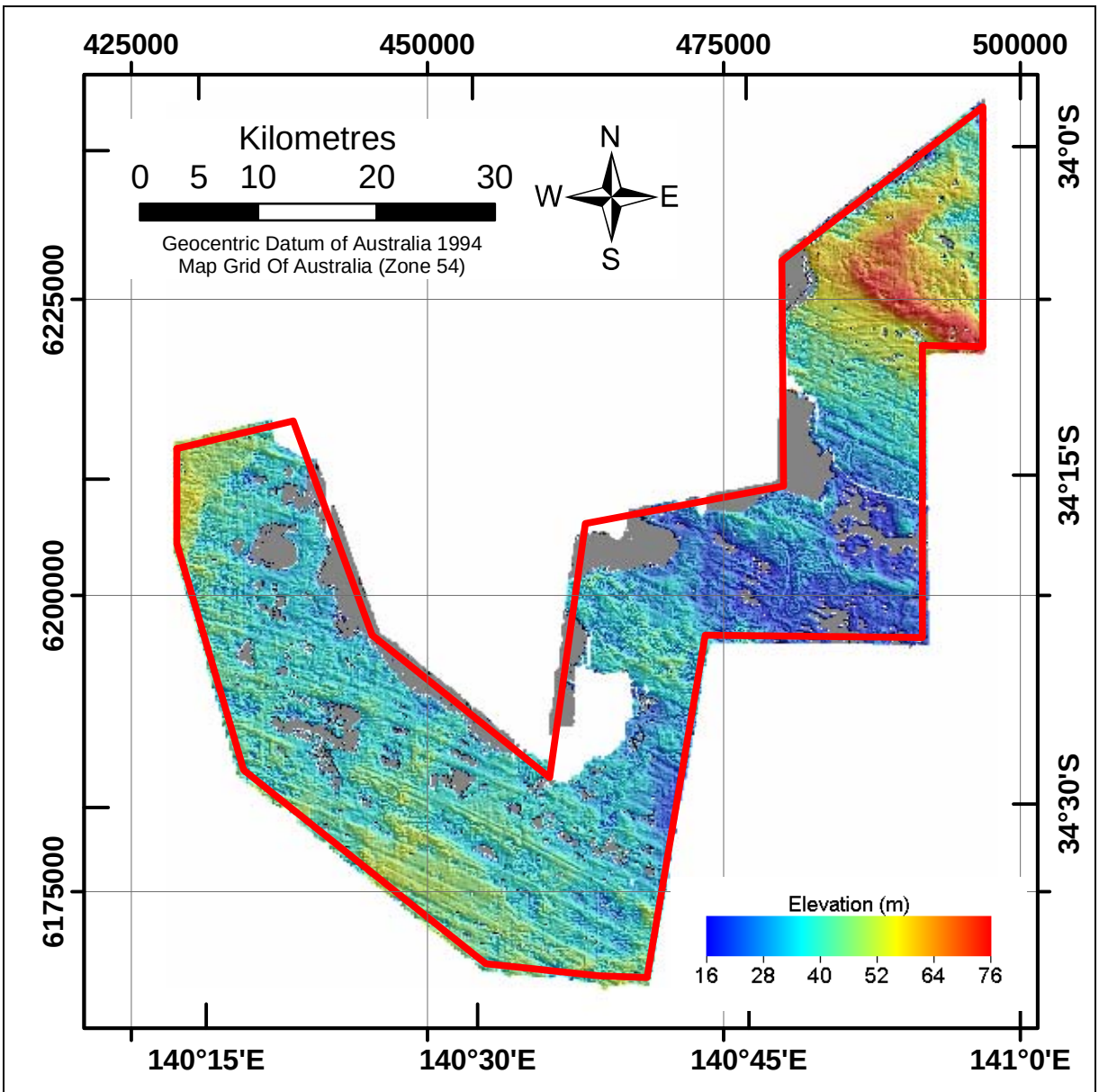

Figure 13.: Elevation of the base of the second (clay) layer. This image has been enhanced with a synthetic sun shade from the north-west.

An image of the elevation of the top of the clay layer is also instructive. Now, although much of the same topography that was apparent in the pervious image remains, the relief has been softened and blurred by the deposition of the Blanchetown Clay. Changes are most apparent on topographic highs rather than lows.

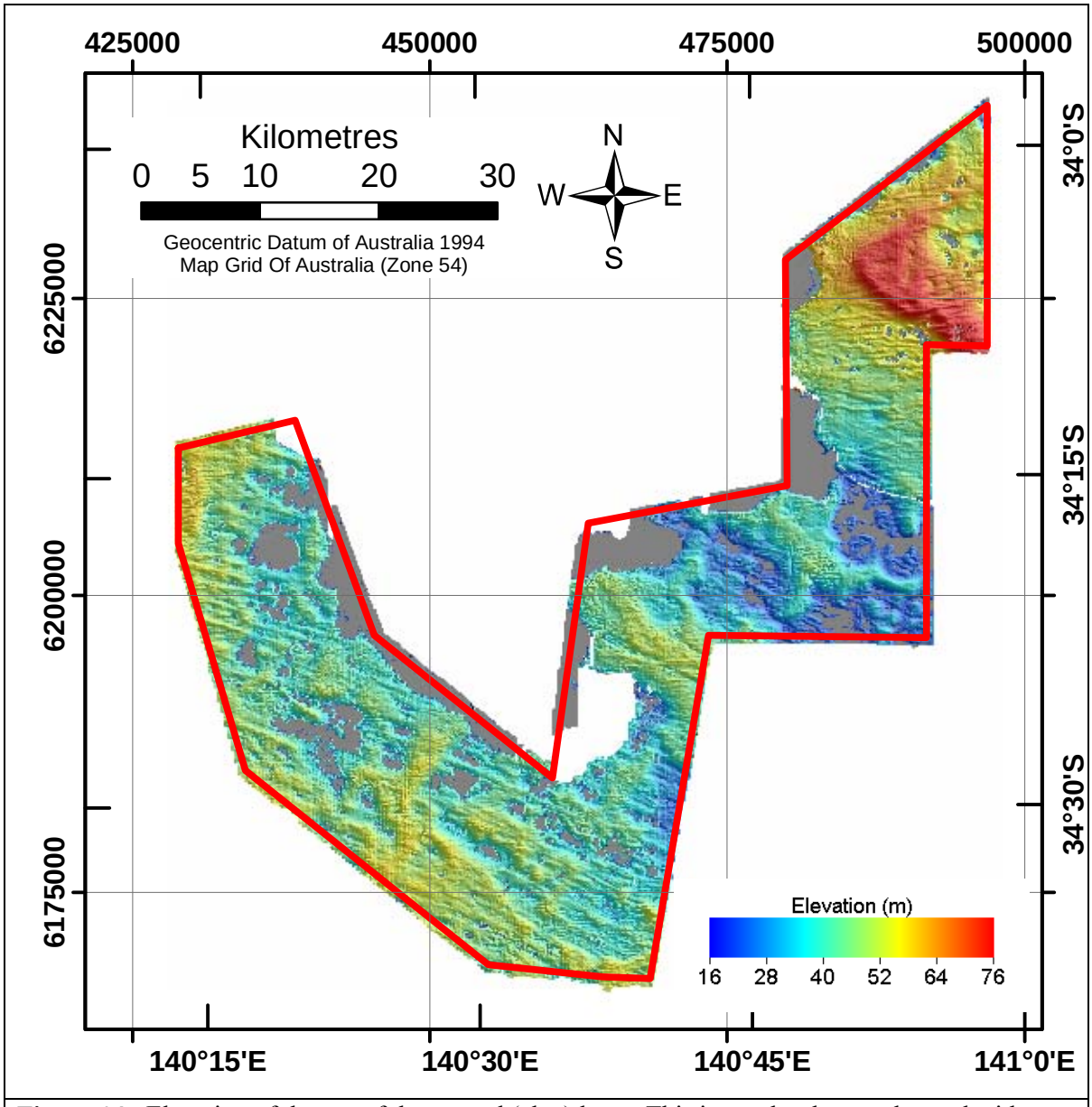

Figure 14.: Elevation of the top of the second (clay) layer. This image has been enhanced with a synthetic sun shade from the north-west.

5.3 Accuracy and Limitations

The images of the last section display convincing patterns that, in many places, accord with our expectations for them. However, geophysical inversion is necessarily non-unique and there is always the danger that we may be achieving this match more as a result of the constraints we have applied than by unbiased assessment of the data. The main objective the survey was to map the Blanchetown Clay and here we must highlight the main potential difficulty that could arise from the inversion process.

In the analysis of all electromagnetic data of this type we must remember that it is always difficult to discriminate a change in layer thickness from a change in its conductivity. Moreover, as the layer becomes thinner, this difficulty increases. Thus, with thin layers, it is difficult to tell if an observed change in electromagnetic response has been caused by a layer thickening or by it increasing in conductivity.

In this case, we set up the inversion with a bias to cause changes in the high frequency data to appear as thickness variations in the clay layer. This was primarily achieved by stopping the clay conductivity from dropping below 100 mS/m and by providing an expectation that the clay conductivity will be approximately 240 mS/m. This is a reasonable enough assumption. After all, we might expect that very low conductivities would be better represented by an absence of clay in favour of either the upper or lower sands.

However these constraints must have influenced the inversion to some extent. A comparison to the clay thickness (Figure 11(b)) and conductivity (Figure 12(b)) images suggests that this might be so. The clay thickness image looks quite "natural". By that we mean that the structures and patterns evident in the image appear to relate to geomorphic features of the landscape. In contrast, while the conductivity image is not completely "unnatural" it does not show the same clarity of pattern as the thickness image. This difference may be indicative of the impact of the clay conductivity constraints.

In addition to the above caveat we should also remember that there may be places where the model that we are fitting does not suit the local geology. An obvious example is Area G, where we modified the parameters of the inversion to suit a small area with a very different geological model. This area was an obvious problem because the general inversion method could not obtain a satisfactory data fit. However, it should be recognized that there may be places where, although the inverted model provides a satisfactory fit, the geological constraints may be inappropriate.

The most obvious situation where this may have occurred is in the NW portion of the Southern Area where the conductive Bookpurnong Beds lie above the water table. In this situation a more appropriate model would be to have three conductive layers instead of two. We did not have a chance to investigate this issue in this project but, assuming that the Bookpurnong was not too far above the water table, it is likely that the inversion would have accommodated the responses by placing the extra conductivity into the "bulge" layer rather than the clay layer.

We have two ways of assessing the performance of the inversion, both involve comparisons with drilling information. The first comparison is between the inversion results and induction logging of nearby drill holes. Figure 15 shows such a comparison for the two holes shown in Figure 9. Here PYP5 has thick near surface clay, apparently in three separate layers, while LH041G may or may not have some clay. The inversion finds a thick section for PYP5 and a thin one for LH041G. Neither inversion accommodates the conductivity bulge (of unknown origin) approximately 10 m above the water table. The inversion finds the "bulge" in LH041G with a smaller one for PYP5.

The extent to which the inversions match other down-hole results can be seen in Appendix 2, where the results for 33 holes are shown. In general the inversion can be seen to match the logs as well as might be expected given the constraints of a simple five-layer model.

The other sources of comparative data are driller's logs. Although they are more numerous, these logs are less reliable than the recent induction logging because they are generally of uncertain provenance and have been collected over a considerable time by many different interpreters. Figure 16 shows a scatter plot of this comparison.

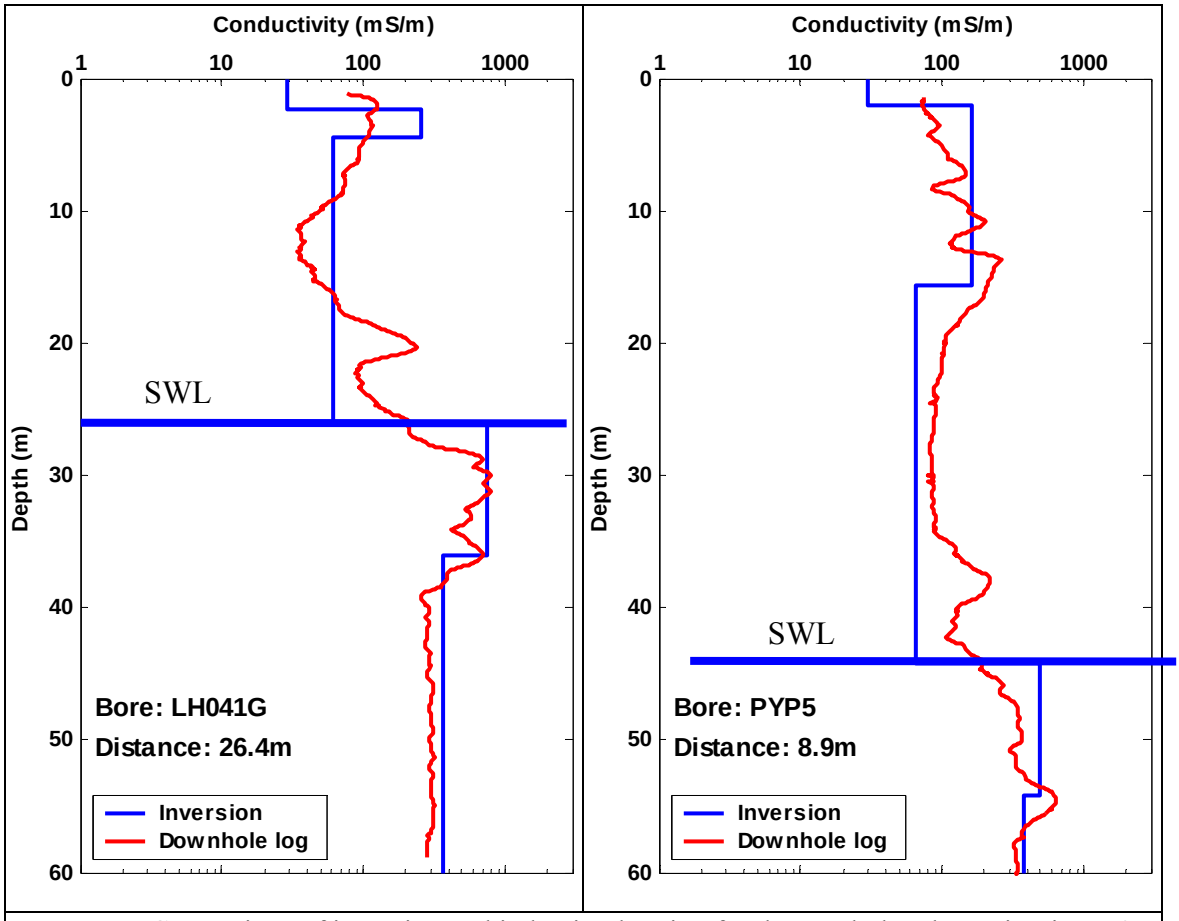

Figure 15.: Comparison of inversion and induction logging for the two holes shown in Figure 9

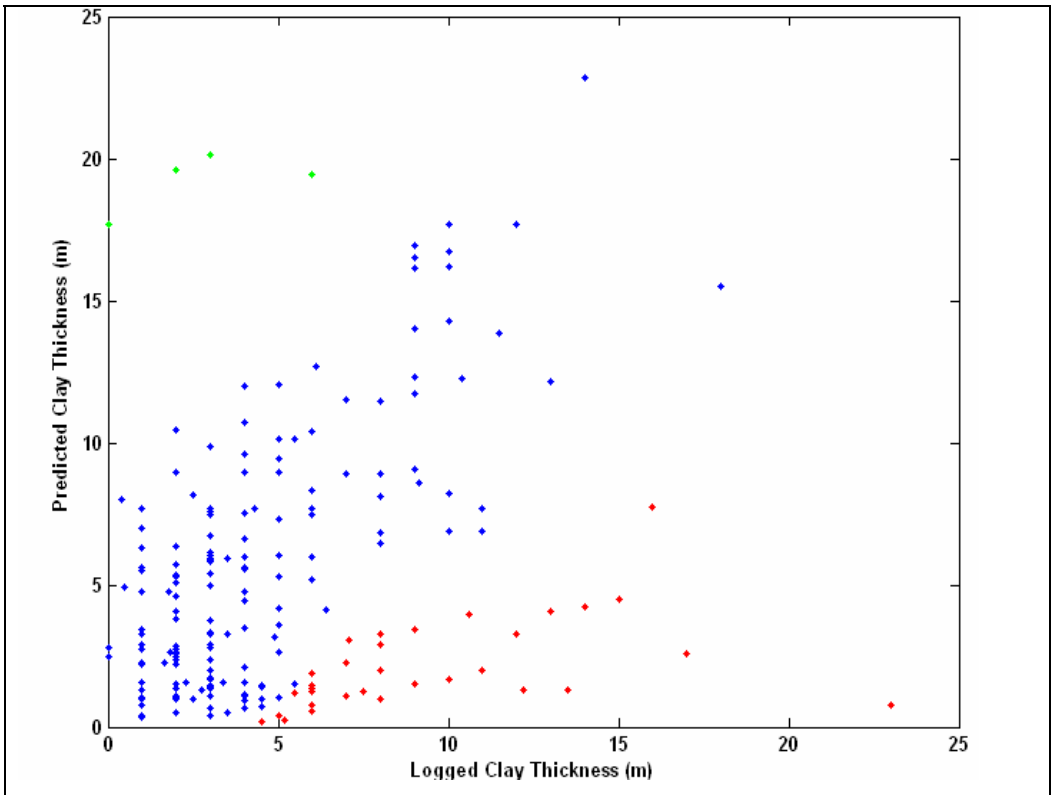

Figure 16.: Scatter plot of clay thickness predicted form the inversion vs that from driller's logs.

There is considerable scatter on this plot. Our assessment is that the points plotted in blue represent the typical scatter for this data set. While those in red and green are probable outliers. The locations of these outliers are plotted on Figure 11(b).

It can be seen that the majority of the red points are either on the very edge of the Murray flood plain or are on the clay-poor, SW slope of the main ridge in the Northern Area. Results close to, or on, the flood plain should be regarded sceptically because the inversion model is inappropriate. The SW slope area is a place of significant disagreement between the HEM results and the drill logs and, to-date, there has not been any opportunity for detailed field checking. However, evidence from two holes drilled as part of recent work (Tan et al, 2003) has suggested that there is very little clay in this area.

The green points are more difficult to explain. Two and perhaps three, of the four are close to boundaries between thicker clays and areas without clay. It could be that the positioning of these holes in error.

However, even accepting these outliers, there is still considerable scatter among the blue points. It would be interesting and useful to investigate the causes for this scatter in greater detail but at this stage we can only speculate about possible causes. Some of these might be:

- *Sampling differences*. Airborne EM systems sample a large area (~2 x flight-height) in comparison with a drill hole. In areas of variable clay thickness substantial discrepancies will occur
- *Positioning differences*. Drill holes are rarely close to flight lines and areas of variable clay thickness will cause differences.
- *Interpretation differences*. The Blanchetown Clay is often has appreciable sand content and interpretation of cuttings may produce quite different logs from those based on electrical conductivity. These problems are multiplied when, as in this case, different people have logged the cuttings over a long period.

6 CONCLUSIONS

The RESOLVE frequency domain HEM system has been used to map the distribution of near-surface clays and in and around the Riverland irrigation districts of South Australia.

After a preliminary analysis to select the optimum system and survey characteristics, approximately 12,000 line-km was surveyed at line spacings of 150 or 300 m. The data was recalibrated with measurements from down-hole induction logs and then inverted using a 1-D layered-earth model. In order to improve the sensitivity to the unknown aspects of the section, the inversion was constrained with as much local geological and hydrological information as possible. These constraints included information about the depth of the water table, the conductivity of the groundwater, the variability of the conductivity and thickness of two sand units and the geomorphic history of the area.

The results of the inversion allow us to reconstruct the strandline-dominated palaeo-topography left when the sea retreated in the Pliocene. They also can be used to define the landscape left after the demise of Lake Bungunnia. This latter surface, defined by the top of the Blanchetown Clay, is a complicated result of fluvial and aeolian redistribution processes that have, in some locations, reworked clays to positions well above the maximum level of the lake.

The resulting detailed map of the distribution of the Blanchetown Clay can be used in a variety of ways.

- It can be used to model the recharge behaviour of the area and assist in the prediction of the future course of salinity inflows to the Murray River.
- If more areas are to be released for irrigation, the map could be used to select areas of thicker clay and inform preferred locations for irrigation.
- Areas of thicker clay are also preferred locations for disposal of saline water from salt interception schemes.

The survey also revealed a hitherto unsuspected, deeper variability in conductivity following the Pliocene strand line pattern. The cause of this pattern is not clear. It could be due to variation in the porosity of Loxton/Parilla Sands or to strandline-correlated variability in the elevation of the contact between the Bookpurnong Beds and the Loxton/Parilla sands.

7 ACKNOWLEDGEMENTS

This project has been part of a larger effort contributing to the South Australian portion of the National Action Plan for Salinity and Water Quality. It would not have been established without the efforts of the individuals who conceived and directed its overall operation. In contrast to many other applications of AEM to salinity problems, this project has been notable because it was designed with clear objectives that could be addressed with appropriate technology. Steve Barnett and Glen Walker we the key movers in this regard.

The authors are also indebted to Richard Lane for his always-wise advice, clear geophysical insights and unflagging support throughout the project.

KP Tan and Steve Barnett provided assistance and relevant geological and hydrogeological constraint information to aid the inversion. Peter Cook and Glen Walker helped in defining appropriate system and survey parameters for the HEM survey. We are also grateful to John Spring and Grant Jones of the BRS for their assistance in acquiring borehole geophysical data used in this study and to Geoscience Australia for providing facilities to conduct the inversion.

This study was made possible through funding support by the South Australian and Commonwealth Governments through the National Action Plan for Salinity and Water Quality, and CRCLEME.

8 REFERENCES

Brodie, R.C., Green A.A., and Munday, T.J., 2003. Constrained inversion of RESOLVE airborne electromagnetic data, Riverland and Tintinara East, South Australia: Data calibration report. CRC-LEME Restricted Report 190R.

Brown, C.M., 1985 Murray Basin, southeastern Australia: stratigraphty and resource potential - a synopsis. BMR report 264

Brown, C.M., and Stephenson, A.E., 1991, Geology of the Murray Basin, Southeastern Australia, BMR Bulletin 235, 430pp.

Cook, P.G., Leaney, F.W and Jolley, I.D., 2001, CSIRO Land and Water Technical Report 45/1, Groundwater recharge in the Mallee region and salinity implications for the Murray River, November 2001

Colwell, J.B., 1977, Stratigraphic drilling of stranded beach ridges, central west Victoria, Unpublished report Australia, BMR geology and Geophysics record 77/61, 19pp

Cowey, D., Garrie, D., and Tovey, A., 2003, Riverland and Tintinara, South Australia, RESOLVE Geophysical Survey, Acquisition and Processing Report. Report to the Bureau of Rural Sciences, available from Geoscience Australia.

Deszcz-Pan, M., Fitterman, D.V., and Labson, V.F., 1998, Reduction of inversion errors in helicopter EM data using auxiliary information, Exploration Geophysics, v. 29, p. 142-146.

Fraser, D., 1978, Resistivity Mapping with an Airborne Multicoil Electromagnetic System: Geophysics, v. 43, 144-172.

Green, A. and Lane, R. 2003, Estimating Noise Levels in AEM Data, Extended Abstracts ASEG 16th Geophysical Conference and Exhibition, February 2003, Adelaide.

Guptasarma, D., and Singh, B., 1997, New digital linear filters for Hankel J0 and J1 transforms, Geophysical Prospecting, 45, 745-762.

Jones, G & Spring, J. 2003 Report on downhole geophysical logging of bores in the Riverland Region, SA for the SA-SMMSP. Bureau of Rural Sciences, Canberra.

Kotsonis, A., 1999, tertiary shorelines of the western Murray Basin: weathering, sedimentology, and exploration potential. AIG Murray Basin Mineral Sands Conference, Mildura AIG Bulletin 26, 57-63

Menke, W., 1989, Geophysical Data Analysis: Discrete Inverse Theory, Academic Press. Section 9.3 p 147

Munday, T., Brodie, R., Green, A., Lane, R., Sattel, D, Cook, P., Barnett, S., and Walker, G. 2003, Developing recharge reduction strategies in the Riverland of South Australia using airborne electromagnetic data – a case study in tailoring airborne geophysics given a particular target and a desired set of outcomes. Extended Abstracts ASEG 16th Geophysical Conference and Exhibition, February 2003, Adelaide.

Roy, P.S., Whitehouse, J., Cowell, P.J., and Oakes, G., 2000, Mineral sands occurrences in the Murray Basin, Southeastern Australia. Economic Geology, 95, 1107-1128

Sandiford, M., 2003a, Geomorphic constraints on the Late Neogene tectonics of the Otway Range, Victoria. Australian Journal of Earth Sciences, 50, 69–80

Sandiford, M., 2003b, Neotectonics of southeastern Australia: linking the Quaternary faulting record with seismicity and in situ stress, eds Hillis, R.R. Muller, D., Evolution and dynamics of the Australian Plate, Geological Society of Australia, Special Publication, 22, 101-113,

Stephenson, A.E., 1986. Lake Bungunnia – A Plio-Pleistocene Megalake in Southern Australia, Palaeogeography, Palaeoclimatology, Palaeoecology, 57 (1986) p 137-156.

Tan, K.P., Munday, T.J. and Leaney, F.W., 2003, The Geochemical, Mineralogical and Petrophysical Characteristics of Sedimentary Materials in the Riverland Region, South Australia, for the Validation of the Helicopter Airborne Electromagnetic Data. CRCLEME Report 154

Wait, J., R. 1982. Geo-Electromagnetism. Academic Press, New York.

APPENDIX 1

The inversion method used here follows Menke (1989). Because the forward model is non-linear the inversion must proceed iteratively. Here each iteration is a complete linear inversion step where the new model parameters defined as follows

$$\mathbf{m}_{n+1}^{est} = \mathbf{m}_0 + \mathbf{G}_n^{-g}\left(\mathbf{d} - \mathrm{g}(\mathbf{m}_n^{est}) + \mathbf{G}_n\left[\mathbf{m}_n^{est} - \mathbf{m}_0\right]\right)$$

where;

$\mathbf{m}_n^{est}$ = Estimated model parameter vector at the n^{th} iteration.

$\mathbf{m}_0$ = Reference model parameter vector.

$\left[\mathbf{G}_n\right]_{ij} = \dfrac{\partial g_i}{\partial m_j}$ = Jacobian matrix at the n^{th} iteration.

$\mathbf{d}$ = Observed data vector.

$\mathrm{g}(\mathbf{m}_n^{est})$ = The forward model at the n^{th} iteration; and

$\mathbf{G}_n^{-g}$ is the so called generalised inverse of the least squares problem given by;

$$\mathbf{G}_n^{-g} = \left(\left[\mathrm{cov}\ \mathbf{m}\right]^{-1} + \mathbf{G}_n^T\left[\mathrm{cov}\ \mathbf{d}\right]^{-1}\mathbf{G}_n\right)^{-1}\mathbf{G}_n^T\left[\mathrm{cov}\ \mathbf{d}\right]^{-1}$$

The covariance matrices [cov **m]** and [cov **d]** contain the model constraint and data noise parameters respectively.

APPENDIX 2

The following plots show the down-hole conductivity measured (with an EM39) and the corresponding inversion results to the airborne data closest to the drill hole. The distance between the airborne sample and the drill hole is given below the drill-hole identification.

These holes were selected because they were within 60m of an airborne sample and went to sufficient depth to achieve a total conductance of 2.1 S. They are basically the same data set that was used to calibrate the RESOLVE system (see Section 2.1) with some additional holes drilled and logged since the calibration was performed.

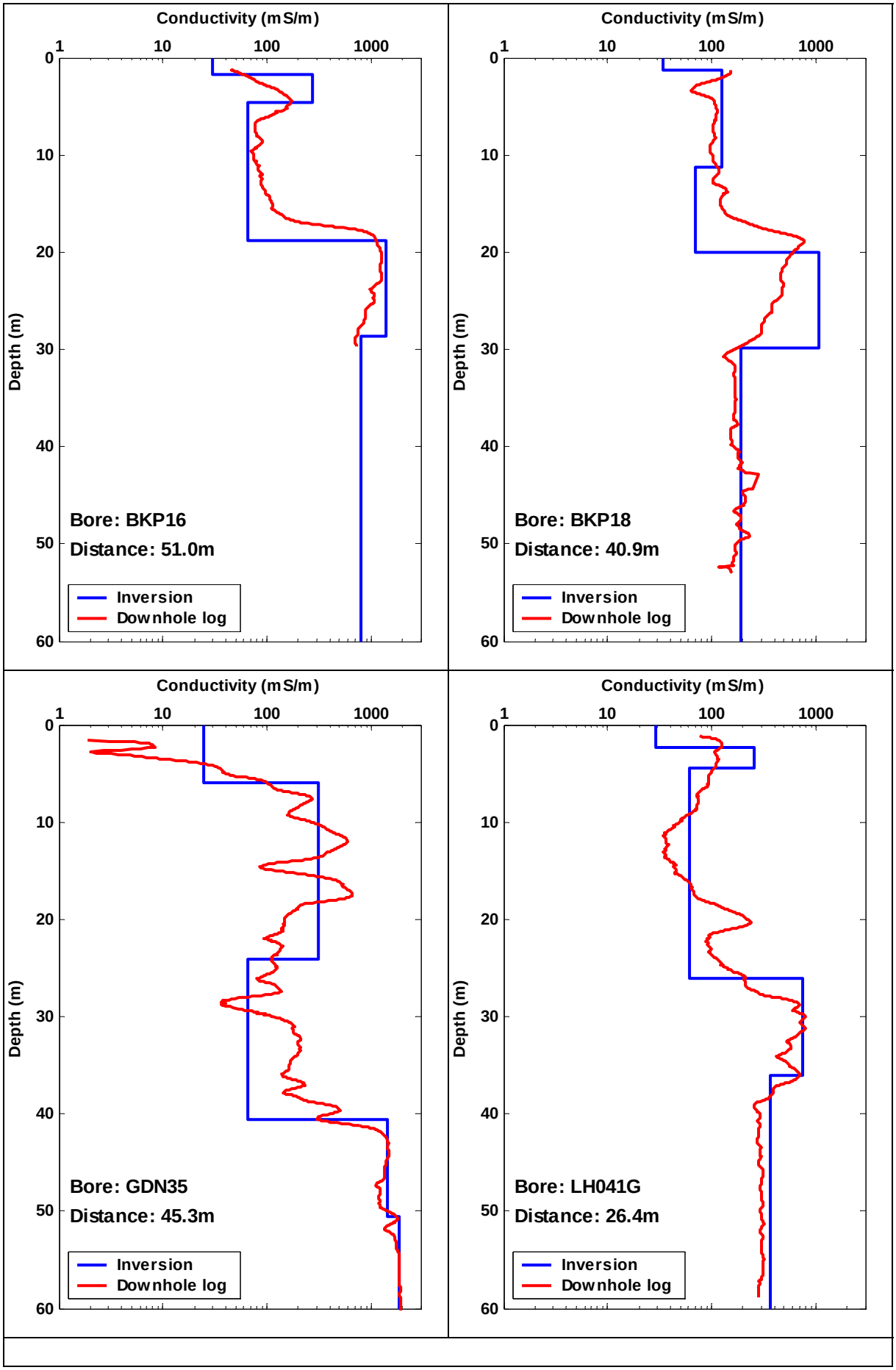
Conductivity (mS/m)
1
10
100
1000
0
10
20
30
40
50
60
Depth (m)
Bore: BKP16
Distance: 51.0m
Inversion
Downhole log
Conductivity (mS/m)
Depth (m)
Bore: BKP18
Distance: 40.9m
Inversion
Downhole log
Conductivity (mS/m)
Depth (m)
Bore: GDN35
Distance: 45.3m
Inversion
Downhole log
Conductivity (mS/m)
Depth (m)
Bore: LH041G
Distance: 26.4m
Inversion
Downhole log

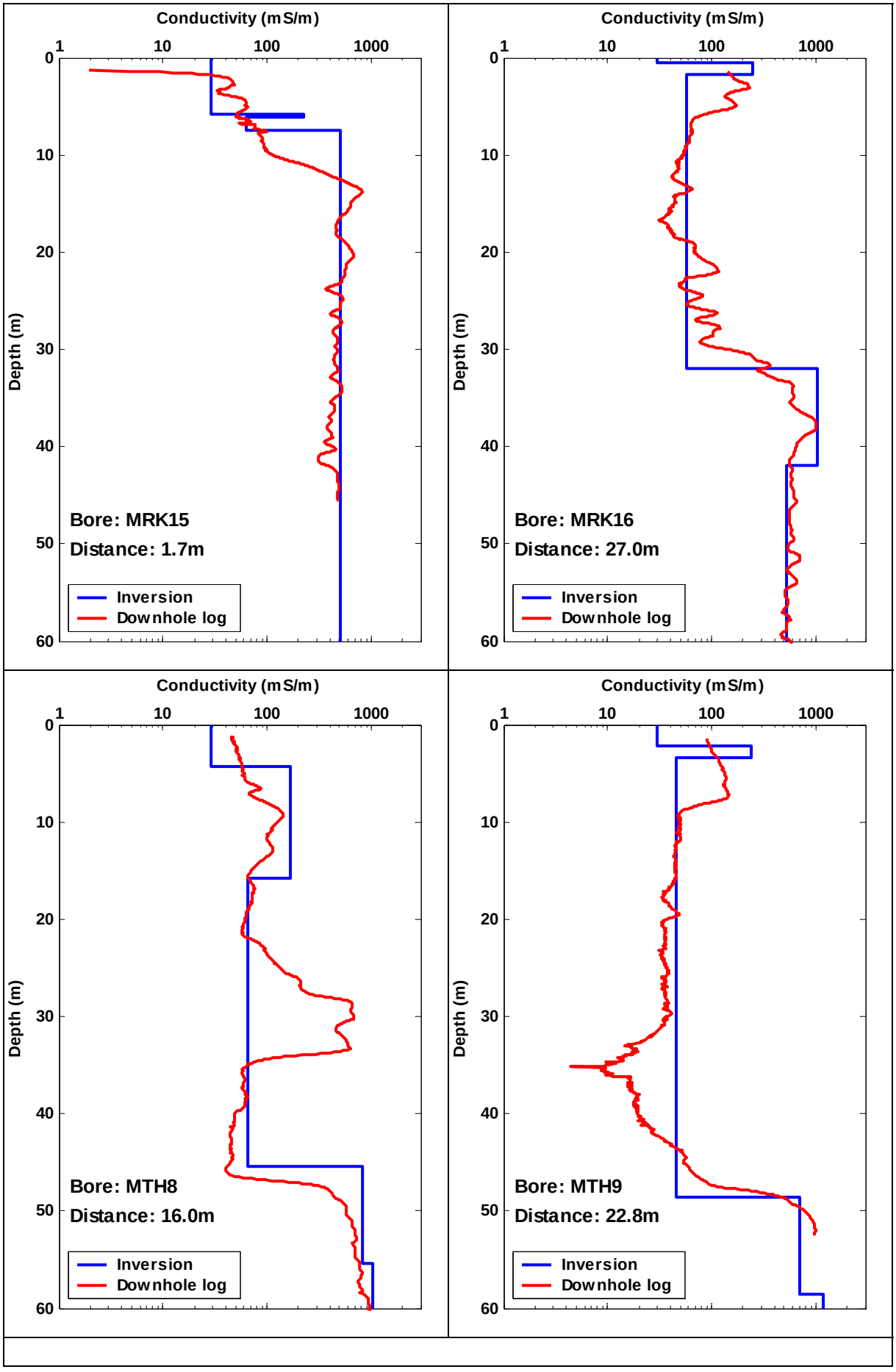
Conductivity (mS/m)
1
10
100
1000
0
10
20
30
40
50
60
Depth (m)
Bore: MRK15
Distance: 1.7m
Inversion
Downhole log
Conductivity (mS/m)
Depth (m)
Bore: MRK16
Distance: 27.0m
Inversion
Downhole log
Conductivity (mS/m)
Depth (m)
Bore: MTH8
Distance: 16.0m
Inversion
Downhole log
Conductivity (mS/m)
Depth (m)
Bore: MTH9
Distance: 22.8m
Inversion
Downhole log

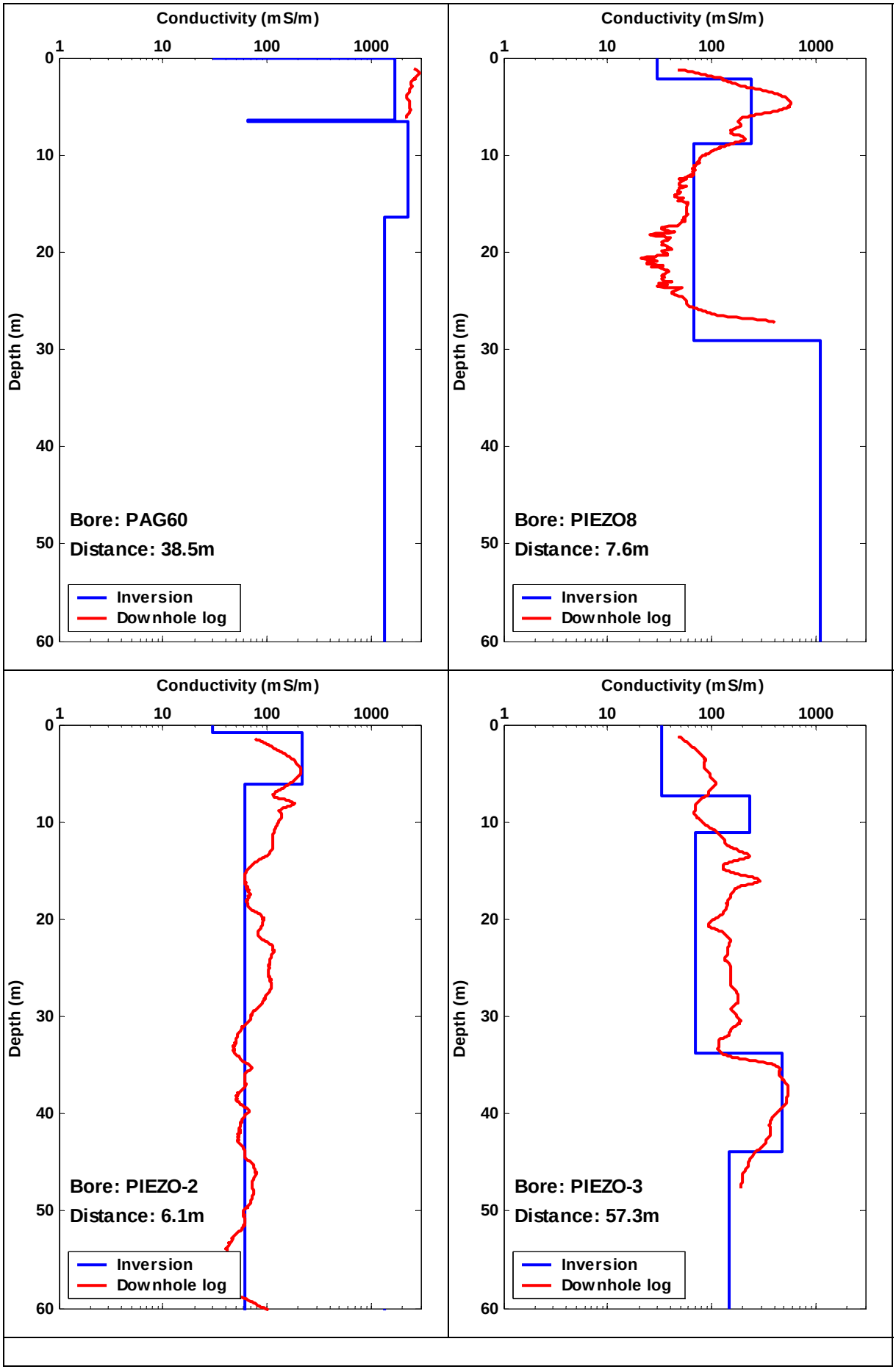
Conductivity (mS/m)
1
10
100
1000
0
10
20
30
40
50
60
Depth (m)
Bore: PAG60
Distance: 38.5m
Inversion
Downhole log
Conductivity (mS/m)
Depth (m)
Bore: PIEZO8
Distance: 7.6m
Inversion
Downhole log
Conductivity (mS/m)
Depth (m)
Bore: PIEZO-2
Distance: 6.1m
Inversion
Downhole log
Conductivity (mS/m)
Depth (m)
Bore: PIEZO-3
Distance: 57.3m
Inversion
Downhole log

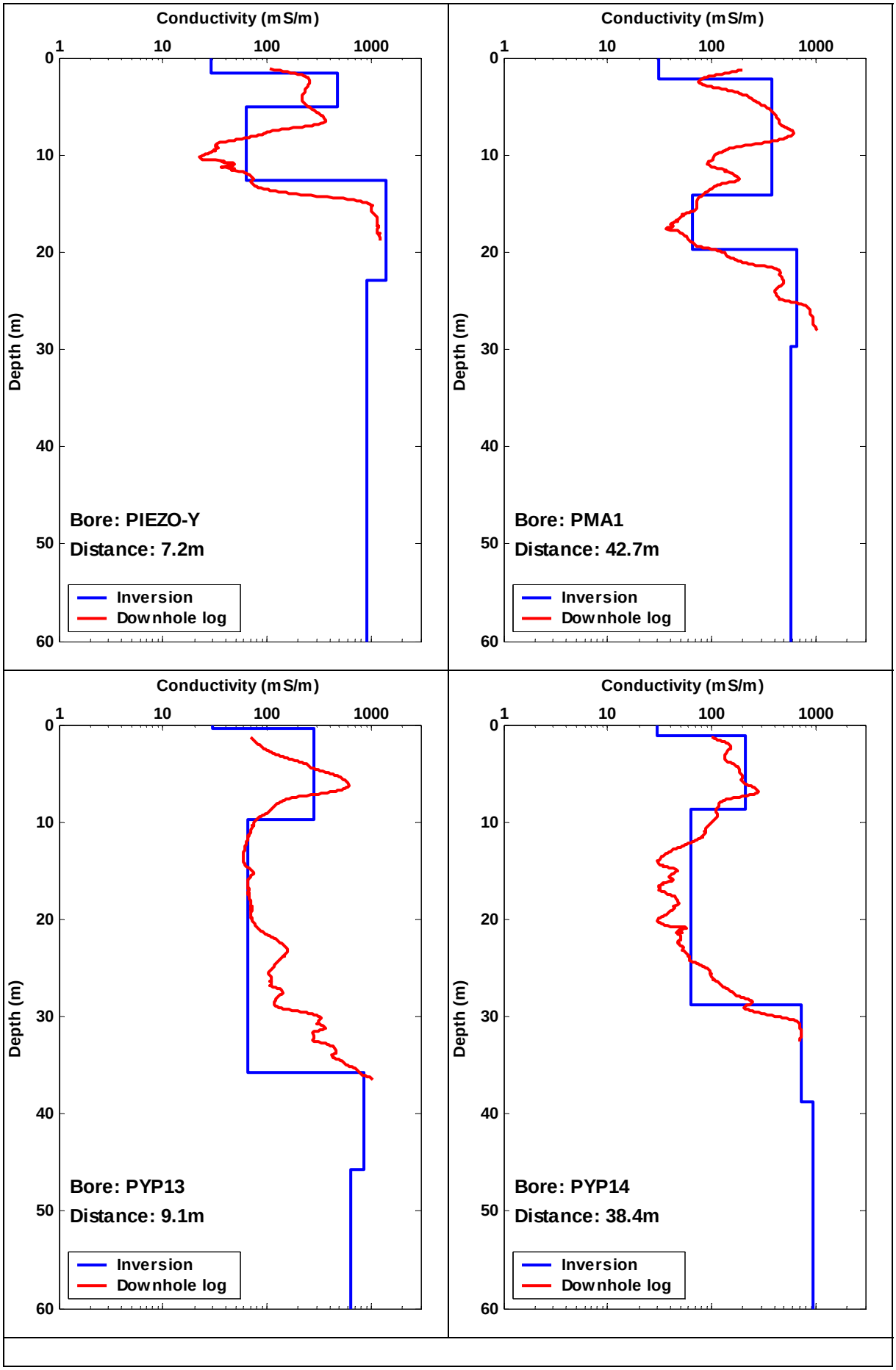
Conductivity (mS/m)
1
10
100
1000
0
10
20
30
40
50
60
Depth (m)
Bore: PIEZO-Y
Distance: 7.2m
Inversion
Downhole log
Conductivity (mS/m)
Depth (m)
Bore: PMA1
Distance: 42.7m
Inversion
Downhole log
Conductivity (mS/m)
Depth (m)
Bore: PYP13
Distance: 9.1m
Inversion
Downhole log
Conductivity (mS/m)
Depth (m)
Bore: PYP14
Distance: 38.4m
Inversion
Downhole log

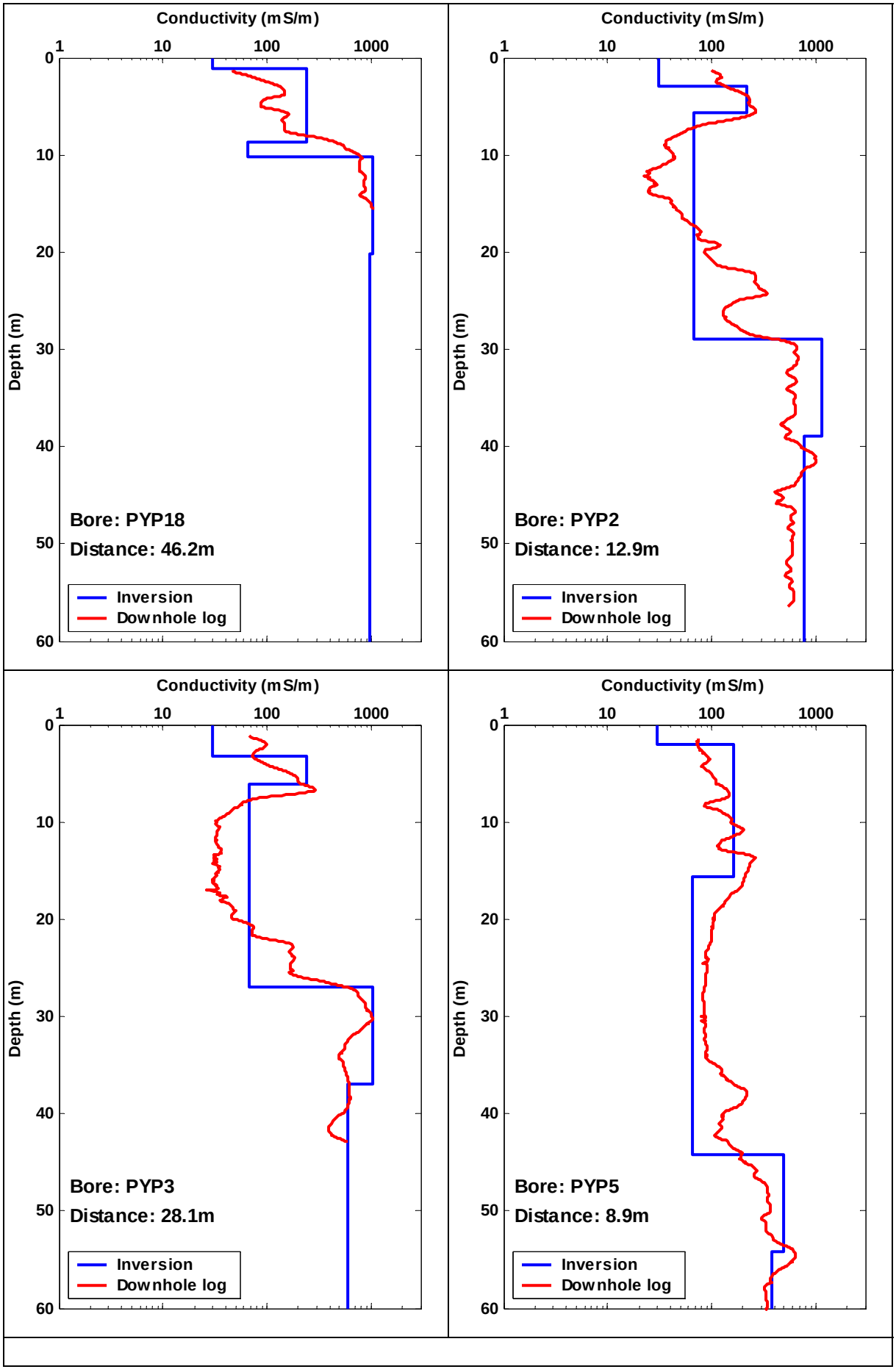
Conductivity (mS/m)
1
10
100
1000
0
10
20
30
40
50
60
Depth (m)
Bore: PYP18
Distance: 46.2m
Inversion
Downhole log
Conductivity (mS/m)
Depth (m)
Bore: PYP2
Distance: 12.9m
Inversion
Downhole log
Conductivity (mS/m)
Depth (m)
Bore: PYP3
Distance: 28.1m
Inversion
Downhole log
Conductivity (mS/m)
Depth (m)
Bore: PYP5
Distance: 8.9m
Inversion
Downhole log

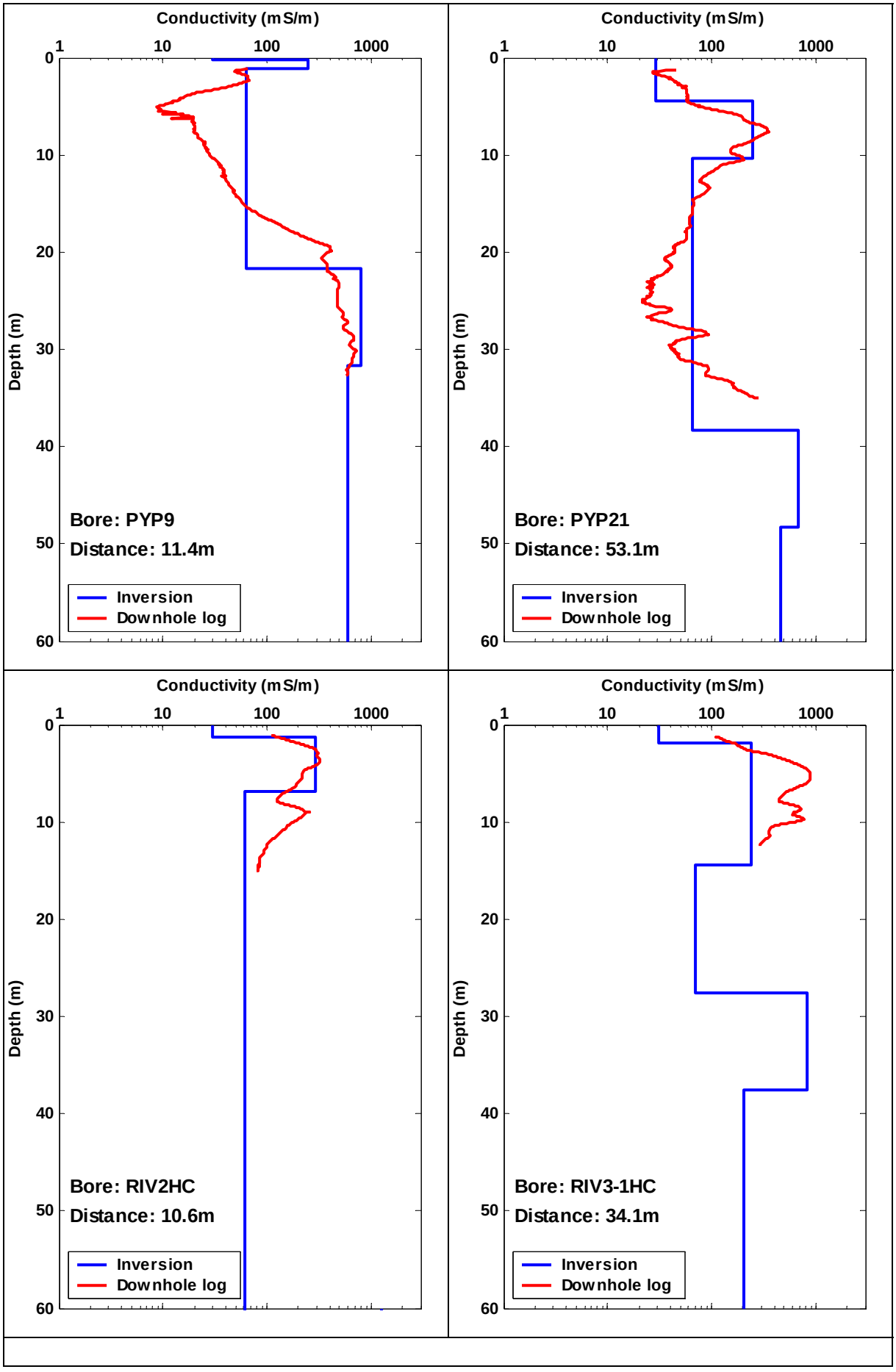
Conductivity (mS/m)
1
10
100
1000
0
10
20
30
40
50
60
Depth (m)
Bore: PYP9
Distance: 11.4m
Inversion
Downhole log
Conductivity (mS/m)
Depth (m)
Bore: PYP21
Distance: 53.1m
Inversion
Downhole log
Conductivity (mS/m)
Depth (m)
Bore: RIV2HC
Distance: 10.6m
Inversion
Downhole log
Conductivity (mS/m)
Depth (m)
Bore: RIV3-1HC
Distance: 34.1m
Inversion
Downhole log

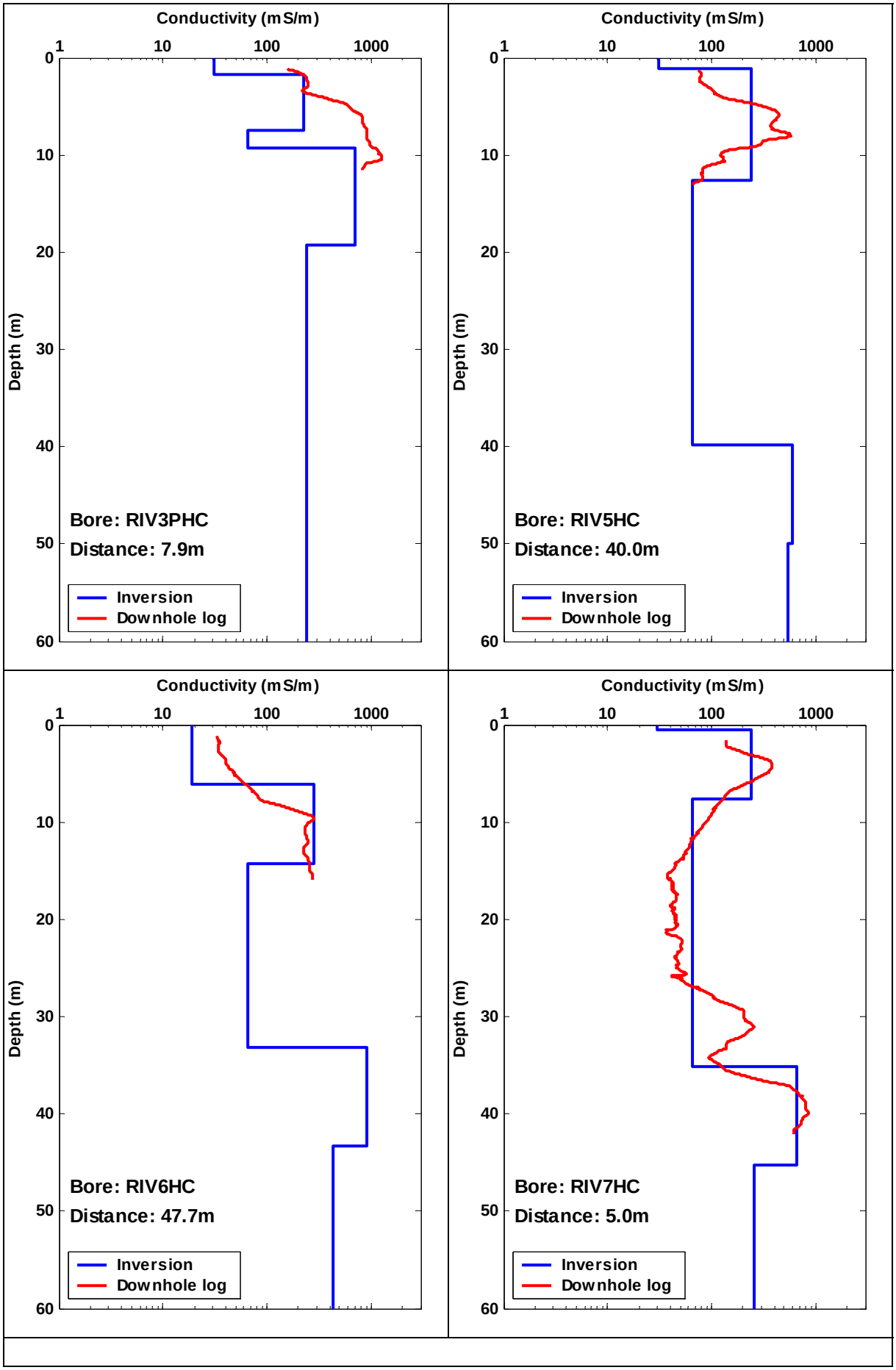
Conductivity (mS/m)
1
10
100
1000
0
10
20
30
40
50
60
Depth (m)
Bore: RIV3PHC
Distance: 7.9m
Inversion
Downhole log
Conductivity (mS/m)
Depth (m)
Bore: RIV5HC
Distance: 40.0m
Inversion
Downhole log
Conductivity (mS/m)
Depth (m)
Bore: RIV6HC
Distance: 47.7m
Inversion
Downhole log
Conductivity (mS/m)
Depth (m)
Bore: RIV7HC
Distance: 5.0m
Inversion
Downhole log

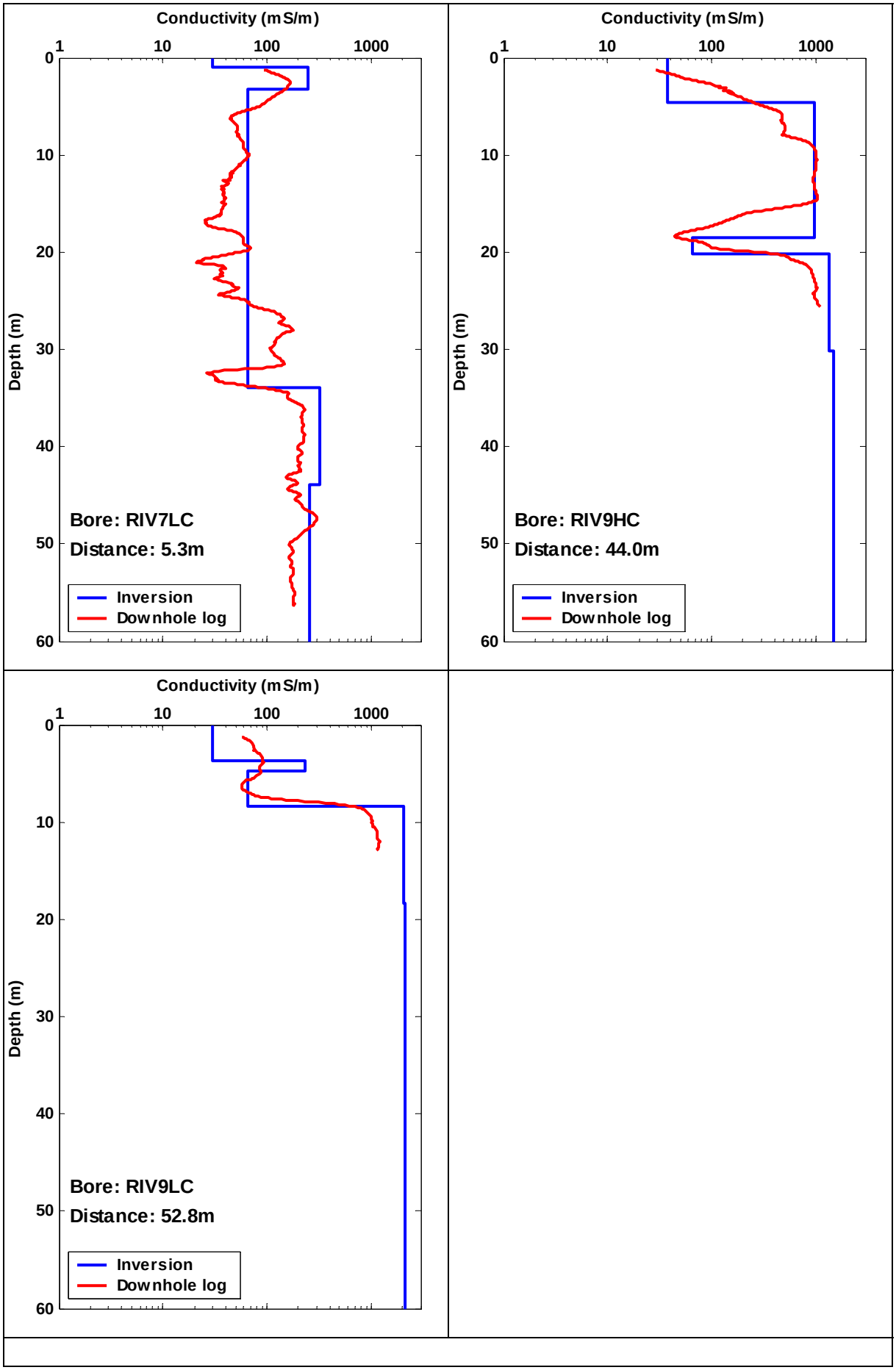
Conductivity (mS/m)
1
10
100
1000
0
10
20
30
40
50
60
Depth (m)
Bore: RIV7LC
Distance: 5.3m
Inversion
Downhole log
Conductivity (mS/m)
1
10
100
1000
0
10
20
30
40
50
60
Depth (m)
Bore: RIV9HC
Distance: 44.0m
Inversion
Downhole log
Conductivity (mS/m)
1
10
100
1000
0
10
20
30
40
50
60
Depth (m)
Bore: RIV9LC
Distance: 52.8m
Inversion
Downhole log

APPENDIX 3

Coordinates of the polygon enclosing the area labelled G on Figure 2.

Vertex Number	Easting (m)	Northing(m)	Vertex Number	Easting (m)	Northing(m)
1	479713	6206043	**23**	482494	6199321
2	480214	6205523	**24**	481974	6198520
3	481074	6205083	**25**	481294	6197900
4	482735	6204583	**26**	481174	6197160
5	483555	6204623	**27**	480654	6196800
6	483515	6204122	**28**	480414	6197480
7	483995	6203502	**29**	479813	6197940
8	484375	6202682	**30**	479113	6197980
9	485095	6202442	**31**	478813	6198520
10	485976	6201381	**32**	478833	6198981
11	486976	6201401	**33**	479453	6199141
12	487256	6200781	**34**	479613	6199581
13	486896	6200241	**35**	479173	6199901
14	485896	6200241	**36**	479933	6200501
15	485135	6199921	**37**	480214	6201702
16	484795	6199141	**38**	480234	6203082
17	484155	6199001	**39**	480074	6203982
18	483915	6199621	**40**	479253	6204523
19	483775	6200081	**41**	479113	6205083
20	483255	6200121	**42**	479133	6205863
21	482294	6200381	**43**	479353	6206203
22	482034	6199761	**44**	479593	6206303